



Technical University of Crete

Department of Production Engineering and Management

**Real-Time Merging Traffic Control for Throughput Maximization at
Motorway Work Zones**

Thesis submitted in partial fulfillment of the requirements for the degree of
Master of Science

by

ATHINA TYMPAKIANAKI

Chania, Greece, 2011

The thesis is approved by the following jury:

Markos Papageorgiou (Supervisor), Professor _____

Ioannis Papamichail (Co-supervisor), Assistant Professor _____

Dimitrios Rovas, Assistant Professor _____

Acknowledgements

I would like to thank my supervisor Professor Markos Papageorgiou for his advice and guidance. His interest, enthusiasm and knowledge made this thesis successful. I also thank my co-advisor Dr. Ioannis Papamichail for his guidance and suggestions. I am also grateful to Professor Dimitrios Rovas who also participated in my thesis committee.

I am also grateful to my fellow researchers, PhD student Anastasia Spiliopoulou and Dr. Anastasios Kouvelas for their valuable contribution, support and patience, which made the accomplishment of this thesis possible. I would also like to thank all the members of the Dynamic Systems & Simulation Laboratory, who have been both colleagues and friends.

Finally, I would like to thank my family and friends for their help and support throughout my studies.

Contents

List of Figures	6
List of Tables.....	8
Abstract.....	9
1 Introduction.....	10
1.1 Scope of the study.....	10
1.2 Thesis outline	11
2 Merging Traffic Control.....	12
2.1 Introduction	12
2.2 Work zone infrastructure	12
2.3 Merge area capacity.....	12
2.4 Control devices.....	13
2.5 Real-time measurements or estimates.....	14
2.6 Control Algorithm.....	14
3 Traffic signal operation policies and the control strategy ALINEA.....	16
3.1 The ALINEA strategy	16
3.2 Traffic signal metering policies	17
3.2.1 One-car-per-green.....	17
3.2.2 <i>n</i> -cars-per-green.....	18
3.2.3 Full traffic cycle	18
3.2.4 Discrete-release-rates	18
4 Microscopic simulator AIMSUN	20
4.1 Introduction	20
4.2 Input parameters	20
4.2.1 Network layout	20
4.2.2 Traffic demand data	21
4.2.3 Traffic control.....	21
4.3 AIMSUN API	21
4.4 Simulation parameters	22
4.4.1 AIMSUN Scenario	22
4.4.2 AIMSUN Experiment.....	22

4.4.3	AIMSUN Replication	22
4.5	Simulation outputs	23
5	Modeling and simulation setup	24
5.1	Network	24
5.2	Demand scenario	25
5.3	Description of the control implementation.....	26
5.3.1	Description of the No-Control implementation.....	26
5.3.2	PI-ALINEA control strategy	26
5.3.3	Investigation of the traffic lights position.....	27
5.4	Micro-simulator AIMSUN	28
5.5	Simulation results and evaluation criteria.....	28
6	Simulation results	29
6.1	No control case	29
6.2	Control strategy PI-ALINEA	34
6.3	Investigation of the position of the traffic lights	39
7	Application of AFT to the merging control strategy	42
7.1	The Adaptive Fine-Tuning (AFT) Algorithm	42
7.2	Application of AFT with AVD as the objective criterion	45
7.2.1	Control scenario 1	45
7.2.2	Control scenario 2	48
7.2.3	Control scenario 3	55
7.2.4	Control scenario 4 with fixed set point	58
7.2.5	Application of AFT with Deviation Error of the regulator as the objective criterion	61
8	Conclusions and future work	66
8.1	Thesis summary.....	66
8.2	Concluding remarks.....	66
8.3	Future approaches	67
	Bibliography	68

List of Figures

Figure 2-1: Typical motorway work zone area.....	12
Figure 2-2: Fundamental diagram of a merge area.	13
Figure 2-3: A general real-time merging traffic control system.....	15
Figure 3-1: The ALINEA local ramp metering strategy.	16
Figure 4-1: Schema of Aimsun API module.....	22
Figure 5-1: Work zone infrastructure dimensions.	24
Figure 5-2: Work zone infrastructure features.	24
Figure 5-3: Demand scenario of the infrastructure.	25
Figure 5-4: The PI-ALINEA control strategy.	27
Figure 6-1: No-control case, 30 th minute of the simulation.	29
Figure 6-2: No-control case, 37 th minute of the simulation.	30
Figure 6-3: No-control case, 50 th minute of the simulation, spill back.	30
Figure 6-4: Number of vehicles in the merge area in the no-control case.....	32
Figure 6-5: Merge area outflow in the no-control case.	32
Figure 6-6: Outflow versus number of vehicles N in the no-control case.....	33
Figure 6-7: Speed at the merge entrance in the no-control case.	33
Figure 6-8: Control case, 37 th minute of the simulation.....	34
Figure 6-9: Control case, 40 th minute of the simulation.....	34
Figure 6-10: Average vehicle delay versus N with and without control.	35
Figure 6-11: Number of vehicles in the merge area with control.....	37
Figure 6-12: Merge area outflow with control.	37
Figure 6-13: Outflow versus number of vehicles N in the control case.	38
Figure 6-14: Speed upstream of the merge area with control.	38
Figure 6-15: Average vehicle delay versus different traffic lights positions.....	40
Figure 6-16: Speed versus different traffic lights positions.	40
Figure 7-1: Working principle of AFT for automatic calibration of LNTCSs.	43
Figure 7-2: Average vehicle delay for control scenario 1.	46
Figure 7-3: K_p parameter for control scenario 1 (1 AFT run).	47
Figure 7-4: K_i parameter for control scenario 1 (1 AFT run).	47
Figure 7-5: N parameter for control scenario 1 (1 AFT run).....	48
Figure 7-6: Average vehicle delay for control scenario 2.	49
Figure 7-7: K_p parameter for control scenario 2 (1 AFT run).	50
Figure 7-8: K_i parameter for control scenario 2.	50
Figure 7-9: N parameter for control scenario 2.....	51
Figure 7-10: Number of vehicles in the merge area (a) before the use of AFT and (b) after the use of AFT.	53
Figure 7-11: Merge area outflow (a) before the use of AFT and (b) after the use of AFT.....	53
Figure 7-12: Outflow versus number of vehicles N (a) before the use of AFT and (b) after the use of AFT.	54
Figure 7-13: Speed upstream of the merge area (a) before the use of AFT and (b) after the use of AFT.	54
Figure 7-14: Average vehicle delay for control scenario 3.	56
Figure 7-15: K_p parameter for control scenario 3.	56

Figure 7-16: K_I parameter for control scenario 3.	57
Figure 7-17: N parameter for control scenario 3.	57
Figure 7-18: Average vehicle delay for control scenario 5.	59
Figure 7-19: K_P parameter for control scenario 5.	60
Figure 7-20: K_I parameter for control scenario 5.	60
Figure 7-21: Standard deviation error for control scenario 1.	62
Figure 7-22: K_P parameter for control scenario 1.	63
Figure 7-23: K_I parameter for control scenario 1.	63

List of Tables

Table 6-1: Average vehicle delay of the network for the no-control case.	31
Table 6-2: Simulation results for $\hat{N} = 11$ veh.....	36
Table 6-3: Speed measurements for the investigated traffic lights positions.....	41
Table 7-1: Comparison of the average vehicle delay (AVD) with and without the application of AFT algorithm.....	48
Table 7-2: Comparison of the average vehicle delay (AVD) with and without the application of AFT.....	51
Table 7-3: Comparison of the average vehicle delay (AVD) with and without the application of AFT.....	58
Table 7-4: Comparison of the average vehicle delay (AVD) with and without the application of AFT.....	61
Table 7-5: Comparison of the average vehicle delay (AVD) with and without the application of AFT.....	64
Table 7-6: Comparison of the average vehicle delay (AVD) with and without the application of AFT for a set of regulator parameters with fixed set-point.....	65
Table 7-7: Comparison of the average vehicle delay (AVD) with and without the application of AFT for a “bad” set of regulator parameters.....	65

Abstract

Work zones on motorways necessitate the drop of one or more lanes which may lead to significant reduction of traffic flow capacity and efficiency, resulting of traffic flow disruptions, congestion creation, and higher risk of accident. In this study, real-time merging traffic control by use of green-red traffic signals is proposed in order to achieve safer merging of vehicles entering the work zone and, at the same time, aiming at maximizing the merge area throughput and reducing the average travel delay.

A particular issue addressed in this research is the investigation of the appropriate distance between the merge area and the traffic lights which leads, in combination with the real-time merging traffic control strategy, to the most efficient merging of vehicles. The control strategy that is applied for signal operation is the ALINEA PI-type feedback regulator. In order to achieve maximum performance of the control strategy, some calibration of the regulator parameters may be necessary. In the aforementioned investigations, the calibration of the regulator parameter values is conducted manually, via the typical trial-and-error method. In an additional investigation, the recently proposed learning/adaptive algorithm AFT is employed in order to automatically fine-tune the regulator parameters.

Simulation experiments with the microscopic simulator AIMSUN, conducting for a hypothetical work zone infrastructure, demonstrate the potential high benefits of the control scheme, i.e. significant increase of the vehicle speed when reaching the work zone entrance, reduction of the average delay, as well as maximization of the exit flow from the merge area. The simulation results from the application of the AFT algorithm show that, if AFT is properly used, the system's performance can be significantly improved even for a well fine-tuned regulator.

1 Introduction

Nowadays, most human activities involve the use of transportation which results in increasing demand for mobility and rapid increase in road traffic demand which eventually leads to the appearance of traffic congestion. The consequences of traffic congestion are vehicles delays, reduced traffic safety, as well as increased environmental problems. Since the expansion of the existing infrastructure or the construction of new is costly and not always feasible, the most efficient approach in order to improve the traffic conditions is the optimal utilization of the existing infrastructure capacity, through the development and implementation of advanced traffic control systems.

1.1 Scope of the study

Work zones are critical areas of urban or motorway networks. Work zones usually require the closure of one or more lanes of the road, in which case the traffic flow needs to merge from a higher number of lanes into a lower number of lanes within a limited space. When the arriving flow reaches or exceeds the downstream capacity, congestion is created in the merge area due to the reduced infrastructure capacity; and an additional, congestion-induced capacity drop appears due to the need for vehicles to accelerate from low speeds within the congestion to higher speeds downstream of the congestion head (Papageorgiou et al., 2008). Work zone management aims at safe working conditions for work-zone workers, as well as, safe and efficient passage of vehicles. In the past, several strategies have been used to improve traffic conditions at work zones, including speed limitations, as well as signing, markings and particular geometric design, see e.g. (Lin et al., 2004), (FHWA, 2005), (Wei and Pavithran, 2006). More recently, real-time merging traffic control was proposed (Lentzakis et. al, 2007), aiming at throughput maximization and minimization of delays in work zones in a similar way as the mainstream traffic flow control concept by (Carlson et al., 2010), albeit by use of traffic lights instead of variable speed limits.

This study continues on the work of (Lentzakis et al., 2007), improving on the utilized control strategy and investigating the most appropriate positioning of the traffic lights when applying real-time traffic control. The distance between the traffic lights and the merge area is crucial as it affects the vehicles' behavior and particularly the acquired speed when approaching the merge area. It is shown that the appropriate location of the traffic lights may improve the results of merging traffic control, as the capacity drop can be reduced or even eliminated in case of proper merging vehicle speed, and this contributes to a more efficient and safe passage through the merge area.

Another issue addressed in this thesis is the calibration of the regulator parameters for the applied control strategy with particular focus on a recently proposed (Kouvelas, 2011) automatic fine-tuning procedure aiming at optimizing the regulator parameters and ensuring best performance of the utilized control strategy.

1.2 Thesis outline

Chapter 2 presents an overview of the work zone control problem. Particularly, the work zone infrastructure, the merge area capacity, the control devices used and the control concept for work zone management are presented. Chapter 3 includes a general description of the traffic signal metering policies and analyzes the metering policy as well as the control algorithm used for the examined problem. The modeling and simulation of the work zone network was carried out by use of the microscopic traffic simulator AIMSUN, which is briefly described in Chapter 4. Following, Chapter 5 presents all features of the examined network including the description of the network, the demand and control scenarios, the traffic lights position, the metering policy employed for the traffic lights settings, as well as the evaluation criteria used to compare the performance of the applied control scenarios. Chapter 6 presents and analyzes the simulation results of the examined work zone infrastructure for the applied control scenarios. In Chapter 7 a brief overview of the learning/adaptive algorithm (AFT) is presented, as well as the application of the algorithm to the control strategy utilized in the examined work-zone problem. The simulation results with the use of AFT are also discussed in this chapter. Finally, Chapter 8 summarizes the results and presents potential future extensions of the current study.

2 Merging Traffic Control

2.1 Introduction

Work zones are crucial areas of the roadways as the lane closures may lead to significant reduction of the capacity and efficiency, with the result of traffic flow disruptions, congestion creation, and high accident risk. This implies the need to promote safe working conditions for work-zone workers, as well as the safety and efficiency of passing vehicles through the work zone area. Both objectives can be achieved by work zone management.

Some already proposed management measures for work zones include speed limitations as well as signing, markings and particular geometric design (Wei and Pavithran, 2006) while a recently proposed measure is real-time control of the arriving flow which aims at maximization of the merge area throughput or, equivalently, minimization of the average travel delay (Lentzakis et. al, 2007).

The basic elements included in a real-time motorway merging traffic control implementation are briefly described in this chapter. In particular, the characteristics of the work zone infrastructure, the control devices to be used, the real-time measurements or estimates needed, as well as the control algorithm to be employed for effective merging traffic control.

2.2 Work zone infrastructure

A typical motorway work zone area is sketched in Figure 2-1. The vehicles arriving on M lanes must change lanes appropriately within the (typically trapezoidal) merge area so as to fit into the μ lanes of the exit (where M is usually higher than μ). The merging procedure may be quite complex in terms of the required vehicle maneuvers especially when the arriving flow is higher than the work zone flow capacity q_{cap} .

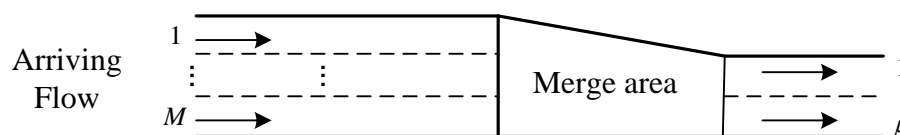


Figure 2-1: Typical motorway work zone area.

2.3 Merge area capacity

The capacity of work zone areas is usually lower than the mainstream motorway capacity due to the drop of one or more lanes at the work zone entrance.

Figure 2-2 displays a typical flow-density diagram for the merge area, where the flow q_{out} is the merge area exit flow and N is the number of vehicles included in the merge area. When N is small, merging conflicts are scarce and swift, while the exit flow is correspondingly low. As N increases, merging conflicts may increase, but q_{out} increases as well until, for a specific initial value N_{cr} , the exit flow reaches the downstream capacity q_{cap} . If N increases beyond N_{cr} , merging conflicts become more serious, leading to substantial vehicle decelerations and eventual accelerations that reduce the exit flow to lower values q_c , where $q_{cap} - q_c$ is the capacity drop due to congestion.

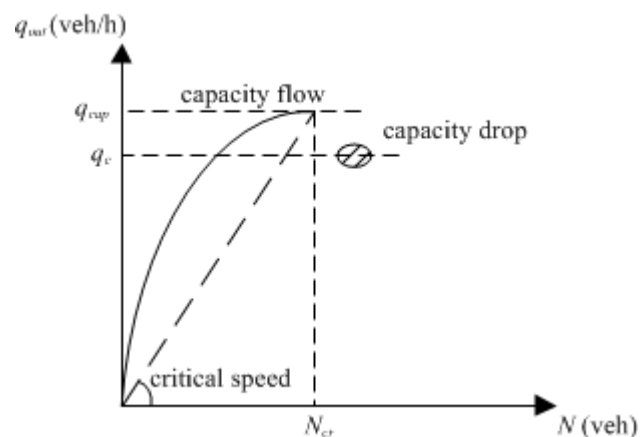


Figure 2-2: Fundamental diagram of a merge area.

Under these conditions, real-time control of the arriving flow may be employed in order to maintain the number of vehicles N in the merge area close to its critical value N_{cr} . This is similar to local ramp metering measures (Papageorgiou and Kotsialos, 2002) where, in contrast, only a part of the arriving traffic flow (i.e. only the on-ramp flow) is controlled so as to maximize the merge area throughput.

2.4 Control devices

Merging traffic control could be applied by use of different control devices aiming at a smooth, safe and efficient merging of vehicles. A possible control device to regulate the arriving flow at work zone areas is traffic lights. A significant issue when applying work zone traffic control is the positioning of the traffic lights position in order to achieve efficient merging of vehicles. More specifically, the traffic lights should be placed sufficiently upstream from the merge area so that the vehicles starting from the traffic lights at low speed, have enough time to reach the appropriate speed for orderly and efficient merging, i.e. a speed that corresponds roughly to capacity flow in Figure 2-2 (critical speed). Traffic lights can be applied to all lanes simultaneously or to individual lanes separately. Recently, Lentzakis et al. (2007) employed real-time merging traffic control at a motorway work zone

infrastructure and achieved a significant increase of the network throughput, considering a specific position of the traffic lights.

The scope of the present research is to investigate the appropriate distance between the traffic lights and the merge area, in conjunction with the control concept implementation.

Other traffic control devices that may be used to control the traffic flow upstream of the merge area are variable speed limits (Carlson et al., 2010), variable message signs by informing the drivers about the congestion ahead and advice them to proceed on specific reactions (e.g. reduce speed, change lane) or via emerging dual vehicle-to-infrastructure communication systems that act directly on individual vehicle speeds.

2.5 Real-time measurements or estimates

In order to apply feedback control so as to maintain the number of vehicles N close to N_{cr} , real-time measurements or estimates of N are needed. This quantity can be directly measured by use of video sensors, but this is not preferable as it may be difficult or costly. The most common way of estimating N , is by use of ordinary loop detectors placed at the appropriate positions in the network (Vigos and Papageorgiou, 2008). Alternatively, one may employ occupancy measurements and target a critical occupancy value o_{cr} (instead of N_{cr}) as in ALINEA ramp metering.

2.6 Control Algorithm

The control algorithm makes use of real-time measurements or estimates of the number of vehicles N or occupancy o in the network in order to maintain $N \approx N_{cr}$ or $o \approx o_{cr}$ which maximizes the merge area exit flow, Figure 2-3.

The feedback algorithm used in this study for merging traffic control is a PI (Proportional-Integral) extension (Wang and Papageorgiou, 2006) of the local ramp metering strategy ALINEA (Papageorgiou et al., 1991; 1997). The control algorithm is activated at each time interval T (in s) and calculates the entering flow $q(k)$ (in veh/h) to be implemented in the next interval k via appropriate operation of the control devices (traffic lights). There are different possible metering policies in order to translate the decision of the control strategy (i.e. the flow (k)) into corresponding traffic light settings. The main characteristics of possible metering policies as well as the detailed description of the feedback algorithm are presented in the next chapter.

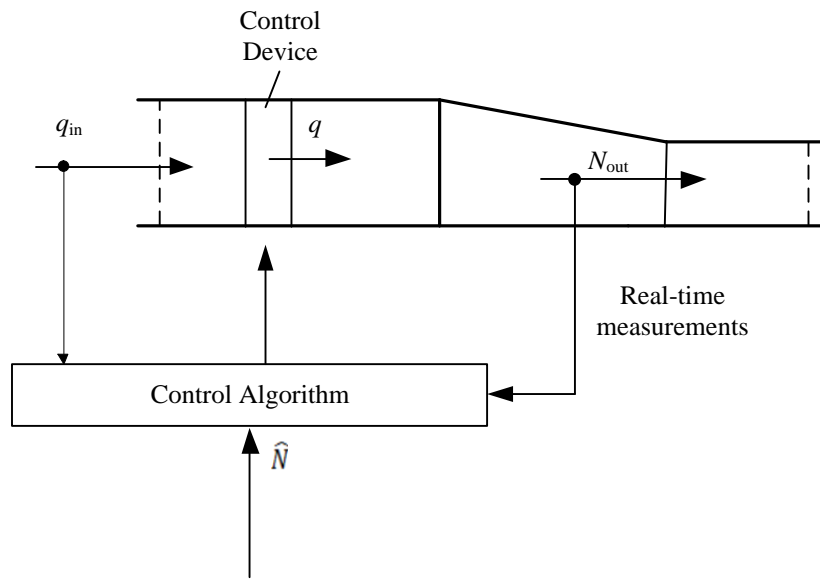


Figure 2-3: A general real-time merging traffic control system.

3 Traffic signal operation policies and the control strategy ALINEA

3.1 The ALINEA strategy

As mentioned in section 2.6, the feedback algorithm used in this study for merging traffic control is an extension of the local ramp metering strategy ALINEA (Papageorgiou et al., 1991; 1997). ALINEA is an integral feedback regulator given by the equation

$$q(k) = q(k - 1) + K_R[\hat{o} - o_{out}(k - 1)] \quad (3-1)$$

where $k = 1, 2, \dots$ is the discrete time index, $q(k)$ denotes the control entering flow to be implemented during the next period k , $K_R > 0$ is a regulator parameter and \hat{o} is a set (desired) value for the downstream occupancy of the motorway. A typical set-value is $\hat{o} = o_{cr}$ in which case the motorway exit flow becomes close to q_{cap} (see Figure 3-1). The same equation can be used if the number of vehicles N is measured, instead of the occupancy percentage.

As mentioned, ALINEA strategy is an integral (I-type) regulator, hence, at a stationary state when the inflow q_{in} remains constant, $\hat{o} = o_{out}(k - 1)$ results from Equation 3.14, independently of the q_{in} value that is not used in the strategy.

The flow value $q(k)$ resulting from (3-2) is constrained within a range $[q_{min}, q_{max}]$ where $q_{min} < q_{cap} < q_{max}$ and is truncated if it exceeds this range. In the next time step the truncated value is used as $q(k - 1)$ in (3-3) in order to avoid the wind-up effect in the I-regulator. ALINEA reacts smoothly even to slight differences $\hat{o} - o_{out}(k - 1)$, thus stabilizing the traffic flow close to the set value (Papageorgiou et al., 1991).

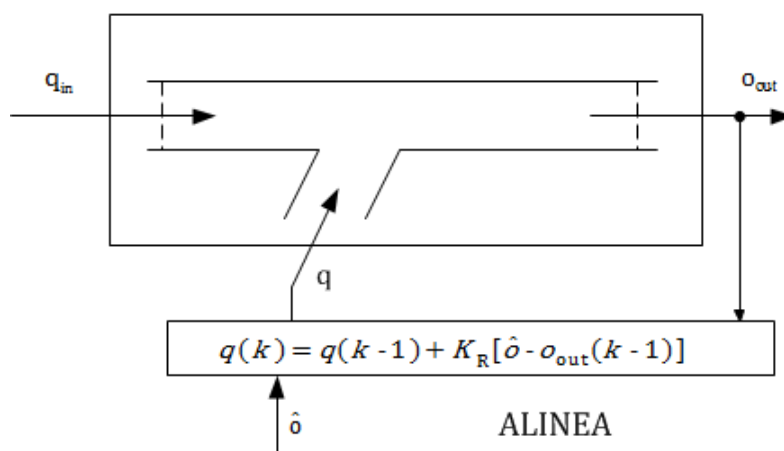


Figure 3-1: The ALINEA local ramp metering strategy.

The described regulator did not perform well in the simulation investigations due to inefficiency of the microscopic simulator. In order to overcome this problem an extension of the ALINEA I-type regulator is used, which appears more reliable for the examined application. Moreover, instead of the occupancy measurements o , the controller uses for its operations the number of vehicles N included in the merge area. Particularly, the extended regulator is a so-called proportional-integral (PI-type) that was proposed (Wang and Papageorgiou, 2006) for the case of freeway stretches with distant downstream bottlenecks and is expressed by the following equation

$$q(k) = q(k-1) - K_P[N(k) - N(k-1)] + K_I[\hat{N} - N(k)] \quad (3-4)$$

where K_P and K_I denote the regulator parameters of the proportional and integral terms, respectively, that must be suitably specified and \hat{N} is a set (desired) value for the downstream number of vehicles.

3.2 Traffic signal metering policies

There are different possible metering policies in order to translate the decision of the control strategy into specific traffic light settings. Some metering policies that were suggested for ramp metering, but can also be applied in merging traffic control in general, are the following: one-car-per-green, n -cars-per-green, full traffic cycle and discrete release rates, but can also be applied (see Papageorgiou and Papamichail, 2008). The selection of the metering policy to be implemented to a particular application depends on its geometrical and traffic characteristics. The flow to be implemented in the next control period T may be distributed equally among the motorway lanes via corresponding individual traffic lights for each lane; while a shift (offset) should be applied for the signal cycle start of each traffic light relative to the cycles of the other traffic lights, so as to enable (to the extent possible) a continuous flow and avoid simultaneous vehicle departures from all lanes (or no departures during red).

3.2.1 One-car-per-green

In this metering policy the green phase G (in s) is fixed (e.g. 2 s), allowing exactly one car to pass at each cycle. Under this metering policy, only the cycle c needs to be calculated. The cycle c (in s) consists of a constant green phase and a variable red phase that allows one vehicle to pass. The implementation of a specific flow q (veh/h) delivered by the control strategy, is translated in real time into a cycle (equal for all lanes) that satisfies

$$q = M \cdot 3600/c \Rightarrow c = 3600 \cdot M/q. \quad (3-5)$$

The cycle length could be rounded off to the next integer value (in s).

The maximum implementable flow q_{\max} under this policy results from

$$q_{max} = \frac{3,600 \cdot M}{(G + R_{min})} \quad (3-6)$$

where R_{min} is the minimum-red constraint to avoid driver confusion.

3.2.2 *n*-cars-per-green

Similarly to the one-car-per-green policy, this policy allows a prespecified number n number of cars to exit per green phase. In this case the real-time translation of an ordered flow value q into a cycle c is obtained from equation

$$c = \frac{n \cdot 3,600 \cdot M}{q} \quad (3-7)$$

and as before the cycle length could be rounded off to obtain an integer value (in s).

The resulting maximum implementable flow now becomes

$$q_{max} = \frac{n \cdot 3,600 \cdot M}{(G + R_{min})}. \quad (3-8)$$

3.2.3 Full traffic cycle

According to the full traffic cycle metering policy, the traffic cycle c is fixed and equal to the metering period T , while the green and red phases are calculated appropriately to implement the ordered flow $q(k)$, with a minimum red phase being considered for safety reasons. The real-time translation of an ordered flow q (veh/h) into a corresponding green phase G (in s) is given by

$$G = \frac{q \cdot T}{S} \quad (3-9)$$

where S in (veh/h) is the saturation flow, with subsequent application of constraints for the green phase G .

3.2.4 Discrete-release-rates

In the *discrete-release-rates* metering policy a range $[q_{min}, q_{max}]$ of permissible flow is defined first and then a number N of discrete flows $q_p \in [q_{min}, q_{max}]$, $p = 1, \dots, N$ is defined via the equation:

$$q_p = q_{min} + \frac{p-1}{N-1} (q_{max} - q_{min}) \quad p = 1, \dots, N. \quad (3-10)$$

Then, the flows q ordered by the control algorithm are rounded off to the closest available discrete flow value q_p (in veh/h) to be implemented. For each discrete flow value q_p , a corresponding signal plan consisting of a specific cycle c_p (in s) and green phase G_p (in s) is predefined such that

$$\frac{G_p}{c_p} = \frac{r_p}{S} \quad (3-11)$$

A full traffic cycle policy is employed here so as to maximize the resulting flow capacity of the traffic lights.

In the case of the motorway work zone infrastructure examined in this research, the essential criteria for the selection of the metering policy are traffic flow homogeneity, as well as the maximum implementable flow. A full traffic cycle policy is employed here so as to maximize the resulting flow capacity of the traffic lights. For the examined infrastructure, the full traffic cycle metering policy is selected for the following reasons:

- ❖ In the two cars per green policy, for a given green phase equal to 4 s so as to allow two cars per green and a minimum-red constraint equal to 2 s and $M = 3$ lanes, the maximum implementable flow resulting from equation (3-6) would be 3600 veh/h, which is very low and much less than the capacity of a motorway infrastructure. Moreover, unnecessary metering delays will occur.
- ❖ The discrete release rates policy would not be suitable for the examined infrastructure, as a high number of discrete release rates N is required in order to achieve sufficiently high flows. Consequently, as the number of discrete values increases, the corresponding cycle and green duration increase as well leading to non-homogeneous traffic flow.
- ❖ In the full traffic cycle policy for a given traffic cycle e.g. 30 s and a minimum red-constraint of 3 s leads to a maximum green $G_{max} = 27$ s, while for a given q_{min} , e.g. 4000 veh/h and a saturation flow of 2000 veh/h, the minimum green resulting from (3-9), is 6 s. The same green phase is implemented at all motorway lanes, albeit with an offset of the cycle start as mentioned earlier. In view of the minimum-red constraint, the maximum implementable flow resulting from (3-9) is 5400 veh/h, which is sufficiently high for a motorway work zone infrastructure.

4 Microscopic simulator AIMSUN

4.1 Introduction

The AIMSUN (Advanced Interactive Microscopic Simulator for Urban and Non-Urban Networks) (TSS, 2009) software includes a microscopic simulator for different traffic networks and the simulation environment AIMSUN NG. It has been designed and implemented as a tool for traffic analysis to assist traffic engineers in the design and assessment of traffic systems.

The AIMSUN simulator follows a microscopic simulation approach during the simulation time in AIMSUN NG environment. This means that the behavior of each vehicle in the network is continuously modeled while it travels through the traffic network, according to several vehicle behaviour models. AIMSUN provides highly detailed modeling of the traffic network and has the ability to model most of the traffic equipment present in a real traffic network like traffic lights, detectors, Variable Message Signs, etc.

The input data required by the simulator is a simulation scenario (Aimsun Scenario), and a set of simulation parameters that define the experiment (Aimsun Experiment). The scenario is composed of the network description, traffic control plans, traffic demand data and public transport plans. The simulation parameters are fixed values that describe the experiment (simulation time, warm-up period, statistics intervals, etc) and some variable parameters used to calibrate the models (reaction times, lane changing zones, etc).

The outputs provided by AIMSUN are continuous animated graphical representation of the traffic network performance, statistical output data (flow, speed, journey times, delays, etc), and data gathered by the simulated detectors (vehicle counts, occupancy, speed).

4.2 Input parameters

Dynamic simulation is characterized by the high level of detail at which the system is modeled. The quality of the model is highly dependent on the availability and accuracy of the input data i.e., the network layout, the traffic demand data and the traffic control.

4.2.1 Network layout

A traffic network model is composed of a set of one-way sections, with specific properties that affect the movement of the vehicles. The sections are connected to each other through nodes (intersections), which may contain different traffic features. In addition, detectors can be included in the model, placed in a desirable

position in the network and be capable to obtain various measurements (number of vehicles, occupancy percentage, speed, density etc). The user can intervene in most of the properties of the features that compose the network.

4.2.2 Traffic demand data

The traffic demand data can be composed of the input flows at the input sections of the network, and the turning proportions at every node of the network. These data can be defined by the user for every different kind of vehicle. Vehicles are generated and input into the network through the input sections, following a random generation model based on the mean input flows for those sections. By default AIMSUN uses exponential distribution. However, other types distribution can be used.

4.2.3 Traffic control

The AIMSUN simulator takes into account different types of traffic control. For intersection control, a phase-based approach is applied in which the cycle of the intersection is divided into phases, where each phase has a particular set of signal groups with right of way at the same time. The units for defining the phases of a control plan are seconds. The duration of a phase determines the duration of the green time of the signal groups assigned to the phase.

During the simulation of a scenario, AIMSUN executes a control plan taking into account the phase modeling for each node. However, this control definition can be variable over the simulation period. The user can employ different plans that will be activated during the simulation at the specified time. Additionally, the user can modify the execution of a control plan by changing the duration of a phase or jumping directly from one phase to another in real-time simulation, which is available via the AIMSUN API (Application Programming Interface).

4.3 AIMSUN API

The AIMSUN API (Application Programming Interface) extends the functions of the simulator as the user can also interact with AIMSUN module during the simulation. This means that the user can employ and evaluate any external application, for example a control strategy, which requires access to internal data of AIMSUN and/or requires dynamic modification of their state.

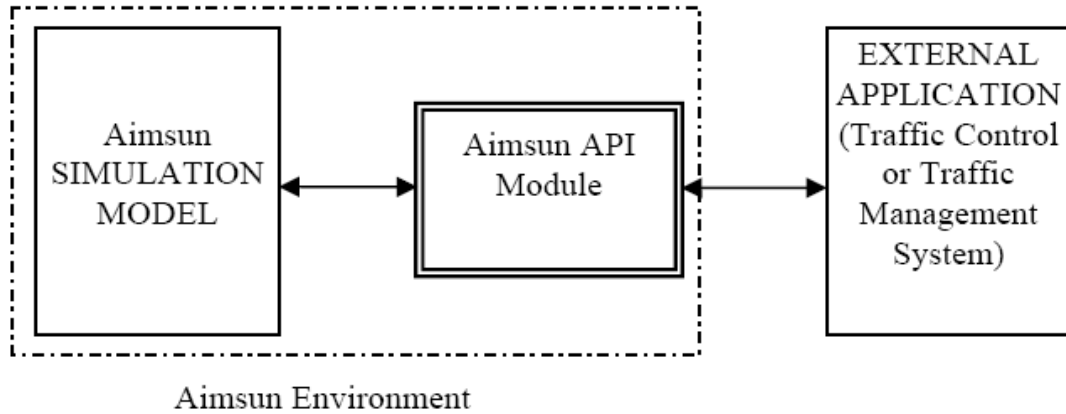


Figure 4-1: Schema of Aimsun API module.

The AIMSUN API (Figure 4-1) is placed, in the functional point of view, between the AIMSUN simulation model and the external application defined by the user. So there are two types of communication processes. On one side there is a communication process between the AIMSUN and the AIMSUN API, which is implemented via AIMSUN NG environment, and on the other side between AIMSUN API and the external application, which has to be implemented by the user, depending on the requirements of the application.

4.4 Simulation parameters

The required information for the preparation and running of dynamic simulation experiments is included in the Scenario (AIMSUN Scenario), the Experiment (AIMSUN Experiment) and the Replication (AIMSUN Replication).

4.4.1 AIMSUN Scenario

The Scenario includes data for the traffic demand, for the public transport plan and the control plans, for the statistical data that will be collected during the simulation, and here the AIMSUN API file is defined, so that it is used for the communication between the user and the simulator in real-time simulation.

4.4.2 AIMSUN Experiment

The Experiment mainly contains information for modeling the movement of vehicles and also here are defined the simulation step, the vehicle's reaction times, the distribution that is used for the production of vehicles in the inputs of the network etc.

4.4.3 AIMSUN Replication

Finally, the Replication is the object to be simulated. For every replication a random seed is used by the simulator. For this reason every replication can give somehow different results.

4.5 Simulation outputs

The microscopic simulator AIMSUN provides the user with several outputs, the main of which are: 2D or 3D graphical animation of the simulation, information on the number of vehicles of every type that cross the network at each simulation time, detailed description of vehicles attributes, representation of the current state of the traffic lights in real time during the simulation run and statistical measures of the traffic state inside the network. Statistical measures, such as vehicle's flow, speed, travel time and delay time, can be specified for the whole system, for each section, for each turning movement or for every stream. Statistical measures such as number of vehicles, occupancy percentages and speed at specific points of the network, are gathered as well from detectors placed at the suitable points.

5 Modeling and simulation setup

This chapter presents the modeling and simulation features of the examined network in the microscopic simulator AIMSUN. Particularly, the geometry and dimensions of the network, the demand and control scenarios, the metering policy employed for the traffic lights settings, as well as the evaluation criterion used to compare the performance of the control scenarios.

5.1 Network

The real-time work zone merging control concept is implemented, via microscopic simulation, at a hypothetical work zone infrastructure consisting of 3 arriving lanes and 2 exiting lanes as depicted in Figure 5-1. The total length of the simulated motorway stretch is 5 km (to accommodate any forming queue length), while the trapezoidal merging area, which is situated 100 m before the end of the motorway stretch, is 50 m long. The capacity q_{cap} of the motorway upstream of the work zone area is sufficiently high to accommodate the investigated demand scenario, while the downstream capacity is reduced due to the lane drop and was found empirically to amount to 5000 veh/h (for a traffic flow including 20% trucks).

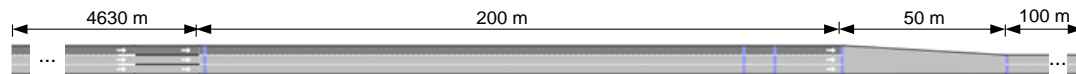


Figure 5-1: Work zone infrastructure dimensions.

Another feature of the described infrastructure is that the left-most lane of the motorway, which is the high-speed lane, is reserved only for cars, while trucks are allowed to use only the other two lanes, as in several real motorways (see Figure 5-2). For the collection of measurements, for operation or evaluation, detectors are placed at different positions along the stretch, as displayed in Figure 5-2.

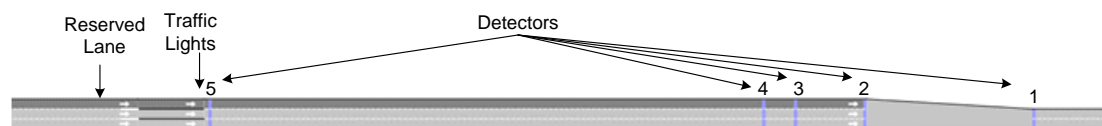


Figure 5-2: Work zone infrastructure features.

5.2 Demand scenario

The control concept was implemented for a representative demand scenario that covers all typical operational states. The duration of the scenario is equal to 2 hours and it follows a trapezoidal profile as sketched in Figure 5-3.

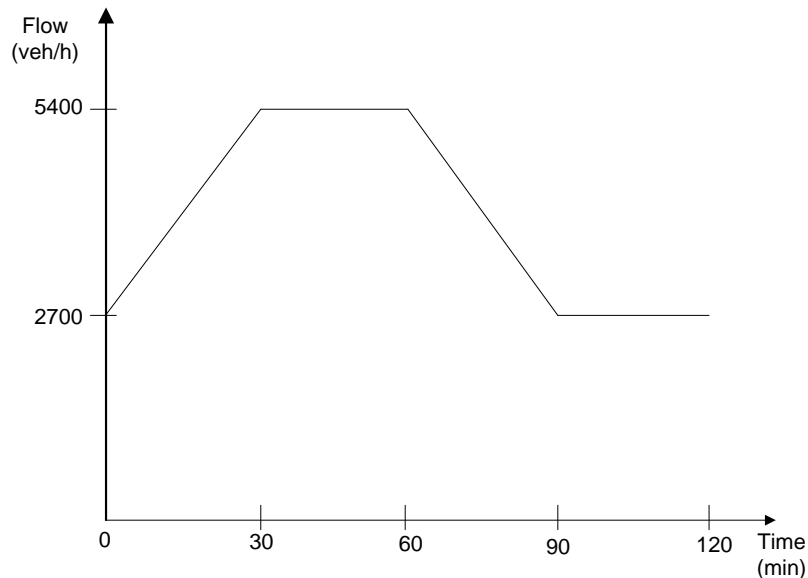


Figure 5-3: Demand scenario of the infrastructure.

The trajectory indicates that in the beginning of the simulation the average demand in the network entrance starts at a low value (50 % of the highest traffic demand) without any traffic flow disruptions or congestion at the work zone merging area. The demand increases gradually within the first 30 minutes, until it reaches a peak demand, i.e., the demand in the peak hour's period, of 5400 veh/h; and remains at this value for the next 30 minutes. During this time period the traffic demand exceeds the merge area capacity q_{cap} which is expected to lead to congestion and reduced efficiency of the infrastructure. During time $t \in [60 \text{ min}, 90 \text{ min}]$, the demand reduces gradually back to the initial low value (50 % of the highest demand) and remains at that value until the end of the simulation. Any queues must be resolved at the end for all scenarios, to obtain comparable results.

The vehicle types included in the demand scenario are cars and trucks. The trucks represent an average of 20% of the total traffic demand and this percentage remains constant throughout the simulation. While determining N for the control algorithm, trucks are counted as equivalent to two cars.

A major concern regarding work zones is the safe passage of vehicles through the merge area. This can be promoted by applying variable or constant speed limits at

specific sections of the network (Carlson et al., 2010) by use of traffic signs. In this study, a speed limit of 80 km/h is applied along the whole motorway stretch.

5.3 Description of the control implementation

Two control concepts are addressed in this research. Firstly, it is considered that no-control is applied at the study area, in order to observe the vehicle merging conflicts, the formation of congestion in the merge area and the capacity drop phenomenon. Then, control is applied, using a PI-ALINEA control strategy, where the values of the regulator parameters are fine-tuned manually via a series of simulation runs. A further investigation was carried out on the optimal values of the regulator parameters, by use of the recently proposed learning/adaptive algorithm AFT (Kouvelas, 2011). A short overview of the algorithm as well as the obtained results for various investigated control scenarios will be discussed in the next chapters. In the following paragraphs, the characteristics of the control scenarios as well as the traffic lights metering policy employed are described.

5.3.1 Description of the No-Control implementation

The first examined case is when no control is implemented to the network. The vehicles entering the motorway exit the work zone without any significant difficulties as long as the arriving flow does not exceed the work-zone capacity q_{cap} . When the arriving flow reaches q_{cap} , the merging operation is not smooth and the vehicles are forced to decelerate due to diverse merging conflicts that inevitably lead to congestion in the merge area. This scenario will then be compared with the control scenarios employed in this study.

5.3.2 PI-ALINEA control strategy

The regulator (equation (5-1)) is activated every $T = 30$ s and receives the real-time measurements of the number of vehicles N included in the merge area, as shown in Figure 5-4, to calculate the entering flow $q(k)$ to be implemented in the next control period k so as to maintain $N \approx N_{cr}$.

The new entering flow to be implemented is not allowed to exceed the range $q \in [4000, 6000]$ veh/h, i.e. a minimum and maximum flow, respectively. Specifically, the minimum admissible flow q_{min} was selected lower than the downstream capacity to enable a sufficient margin for regulator action; for the same reason the maximum admissible flow q_{max} was selected sufficiently large and higher than q_{cap} .

The specification of appropriate regulator parameter values was conducted manually, via trial-and-error. Specifically, various sets of values were tested through a series of simulation runs considering a specific position of the traffic lights. Firstly, the proportional term K_p is tuned and the integral term K_i is set equal to zero. More specifically, the starting value for K_p is a low value in order to have system

stability and then K_P is increased until an acceptable overshoot is obtained. Then, after K_P is obtained, K_I is increased from zero until the overshoot is excessive.

Given that ALINEA, especially the PI-type used in this study, is not particularly sensitive to the distance between the measurement point and the control device thanks to its feedback structure, the parameter values resulted from this investigation should work equally well for other traffic lights positions as well.

In order to specify the appropriate traffic lights position, a primary investigation was conducted, using a fixed flow rate for the traffic lights and setting the traffic lights at different locations upstream of the work zone area, from 50 m up to 300 m in steps of 50 m. The distance for which vehicles had enough time to acquire a speed close to the critical value, before reaching the merge area was around 200 m. Therefore, all the regulator fine-tuning experiments were conducted by positioning the traffic lights 200 m upstream from the merge area (Figure 5-2). Note that a more detailed investigation on the optimum traffic lights location in combination with real time control is presented in the next chapter.

After the experimental investigations, the derived parameter values of K_P and K_I used in this scenario are 150 h^{-1} and 6 h^{-1} , respectively. The identification of the critical value for the number of vehicles in the merge area \hat{N} was also conducted experimentally. The detailed procedure as well as the corresponding results will be described in the next chapter.

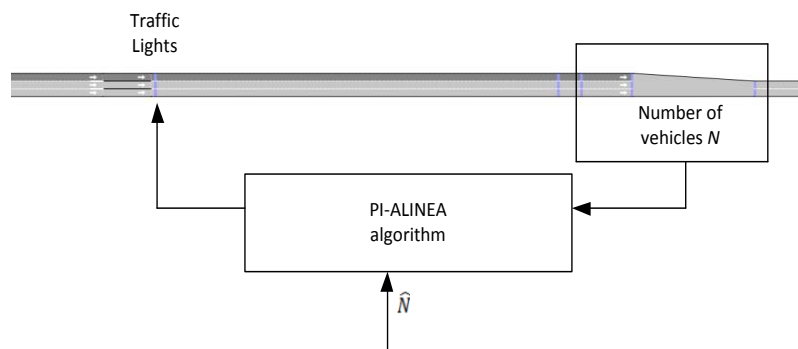


Figure 5-4: The PI-ALINEA control strategy.

5.3.3 Investigation of the traffic lights position

As mentioned in Chapter 2, the investigation of the appropriate distance between the traffic lights and the merge area constitutes one of the main tasks in this thesis. After the identification of the optimal control strategy parameter values, the

proposed control concept is applied to the network considering various traffic light positions upstream of the work zone area. Then, the corresponding results are evaluated according to the performance criteria in order to specify the most appropriate traffic lights position.

5.4 Micro-simulator AIMSUN

The described infrastructure was simulated by use of the microscopic simulator AIMSUN v.6.0.6. (TSS, 2009), using the simulator's default parameters and a simulation time step of 0.1 s. The implementation of the control strategy PI-ALINEA was done via the AIMSUN API (Application Programming Interface) that allows the user to emulate a real-time control environment. Specifically, the simulator delivers in every control period T the number of vehicles N (Figure 5-4). Based on these measurements the control software calculates the corresponding traffic light settings and returns them to the micro-simulator for application.

Since AIMSUN simulator's models are stochastic, different replications with different random seeds may produce different results. For this purpose, 10 replications with different random seeds were carried out for each examined scenario.

5.5 Simulation results and evaluation criteria

During the simulation of the network, real-time measurements are collected (e.g., vehicle's flow and speed measurements) at the locations where detectors are placed. These measurements are not needed by the control strategy but are being used in order to assess the overall performance of the applied control strategies.

In this research the average vehicle delay (AVD) (in s/veh/km) is chosen as the main evaluation criterion. The AVD of the network is delivered by AIMSUN at the end of the simulation by calculating it via the equation below

$$AVD_{sys} = \frac{\sum_{i=1}^{N_{sys}} AVD_i}{N_{sys}}$$

where AVD_i is the average delay time per km of the i -th vehicle and N_{sys} is the total number of vehicles that exit the system during each simulation time step for the whole simulation period.

6 Simulation results

This chapter presents the simulation results of the investigated work zone infrastructure. Microscopic simulator AIMSUN is used for the investigation of the control scenarios applied to the hypothetical motorway stretch described earlier in section 5.1.

In the following two paragraphs the simulated results for the no-control scenario and the implementation of the control strategy ALINEA are presented. As mentioned earlier, the micro-simulator AIMSUN is stochastic thus different simulation runs with different random seeds may lead to different results. For this reason, it is common to use a number (10 in this research) of replications for each investigated scenario and then calculate the average value of the 10 replications for each evaluation criterion in order to compare the different scenarios.

The last paragraph of this chapter describes the investigation of the appropriate traffic lights position and how the distance between the traffic lights and the work zone area may affect the vehicles' behavior as well as the total system delay.

6.1 No control case

In the no-control case, the arriving vehicles enter the merge area and exit without any serious problem as long as the arriving demand is low (Figure 6-1). When the demand increases (peak hours), beyond the work zone capacity, vehicle merging conflicts are observed that lead to vehicle decelerations and formation of congestion (Figure 6-2). Congestion spills back several kilometers, Figure 6-3, but without reaching the simulated network entrance.

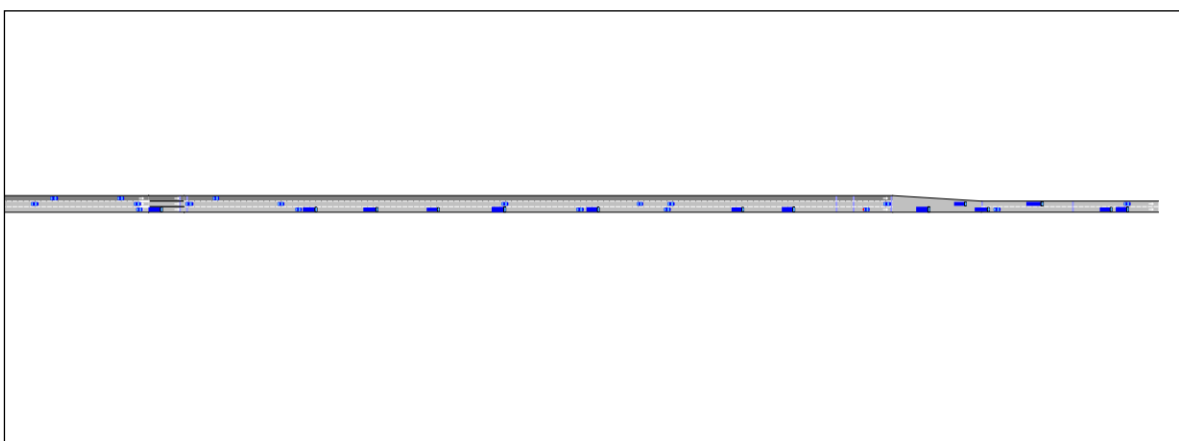


Figure 6-1: No-control case, 30th minute of the simulation.

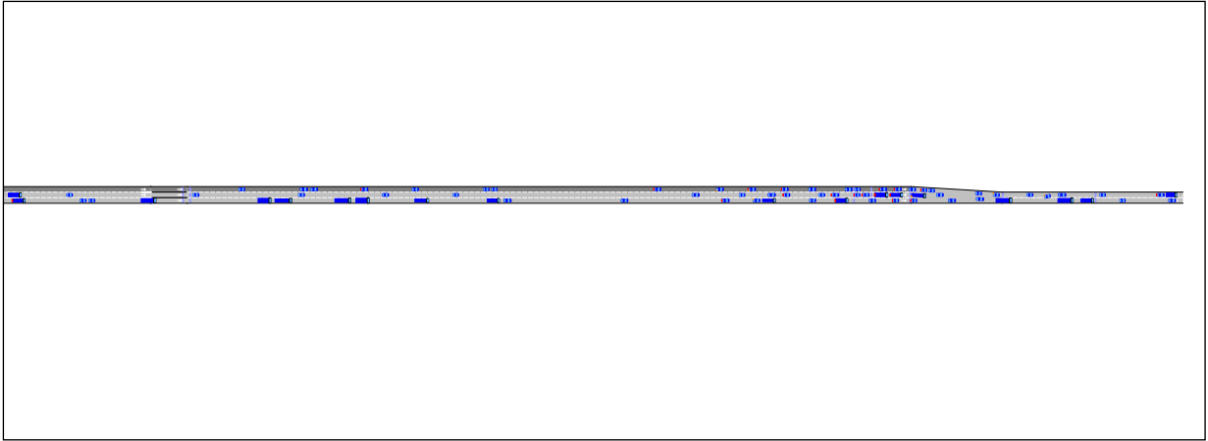


Figure 6-2: No-control case, 37th minute of the simulation.

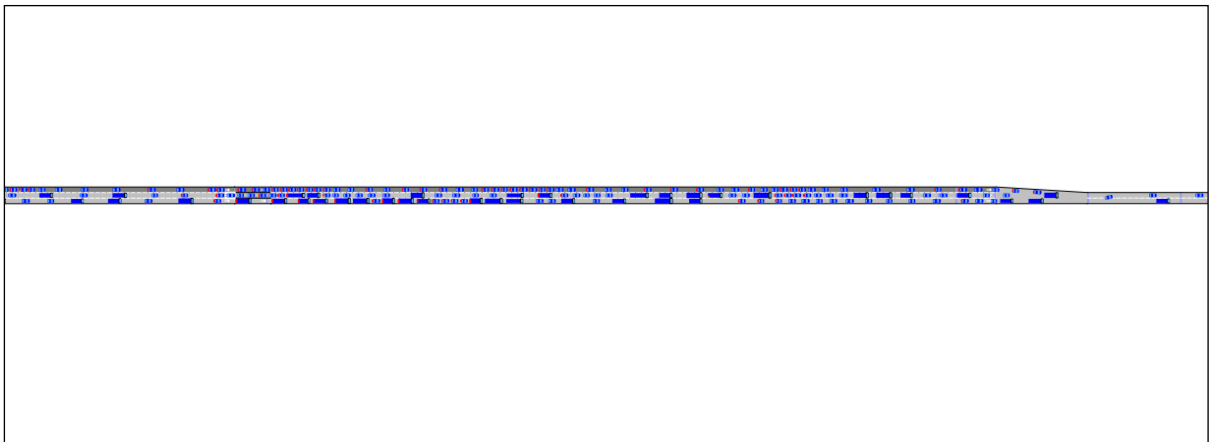


Figure 6-3: No-control case, 50th minute of the simulation, spill back.

Table 6-1 shows the results for the average vehicle delay (AVD) (in s/veh/km) for 10 replications as well as the corresponding minimum and maximum AVD values in the no-control case. As observed in Table 6-1 the resulting mean AVD value is 38.1 while the minimum and maximum values are 24.7 and 51.7, respectively. These results will be later compared to the corresponding results of the examined control scenarios.

The trajectories in Figures 6-4 and 6-5 indicate the number of vehicles in the merge area (see Figure 5-4) and the merge area outflow q_{out} , respectively, for Replication 7 (R7) with corresponding AVD of 37.97, which is close to the mean AVD of the 10 replications. The outflow measurements for all the simulation experiments are collected downstream of the merge area (position 1 in Figure 5-4), with the trucks counted equal to two cars. It is observed that until about $t=40$ min, the number of vehicles in the merge area is slowly increasing (as a consequence of the increasing demand), while the merge area outflow is seen to follow the increase of arriving demand reaching approximately 6300 veh/h in average. After $t=40$ min, the number of vehicles in the merge area increases steeply due to serious merging conflicts that lead to a speed breakdown, and this congested traffic situation becomes stationary until $t=110$ min. The outflow during this time period is reduced

After $t = 110$ min, when the queue dissolves, the number of vehicles in the merge area is seen to drop, and the outflow reduces to lower values due to the decreased demand.

Figure 6-6 displays the merge area outflow versus the number of vehicles as well as the corresponding average flow values for every number of vehicles (blue line). For readability, the time step of the displayed measurements is equal to 1 min. It is observed that for number of vehicles N around 10 the outflow q_{out} reaches its maximum value, which is in average 6300 veh/h. Higher values of the number of vehicles N lead to lower exit flow values due to congestion and capacity drop. Figure 6-7 displays the vehicle speed measurements collected upstream of the merge area, at detector 4 in Figure 5-4. It is observed that during the maximum traffic demand (peak hours) there is a serious speed drop down to around 20 km/h in average, while in the rest of the simulation horizon the average vehicle speed is around 82 km/h. The corresponding results of the other replications are similar to these described above.

Table 6-1: Average vehicle delay of the network for the no-control case.

Replication	Delay Time (s/veh/km)
1	35.13
2	41.45
3	40.85
4	33.82
5	28.90
6	51.52
7	37.97
8	35.32
9	51.77
10	24.75
Average Value	38.15
Minimum Value	24.75
Maximum Value	51.77

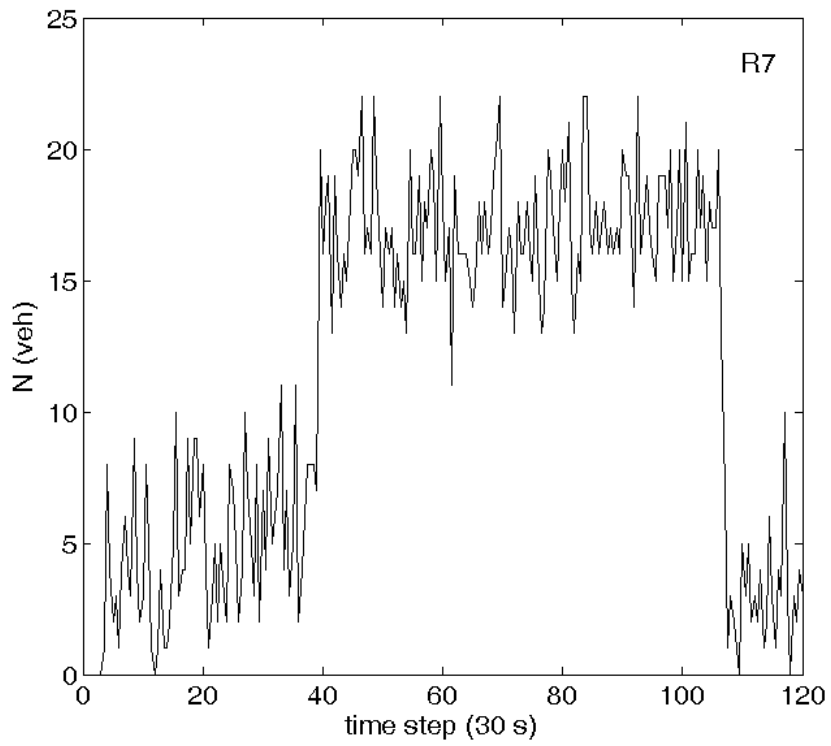


Figure 6-4: Number of vehicles in the merge area in the no-control case.

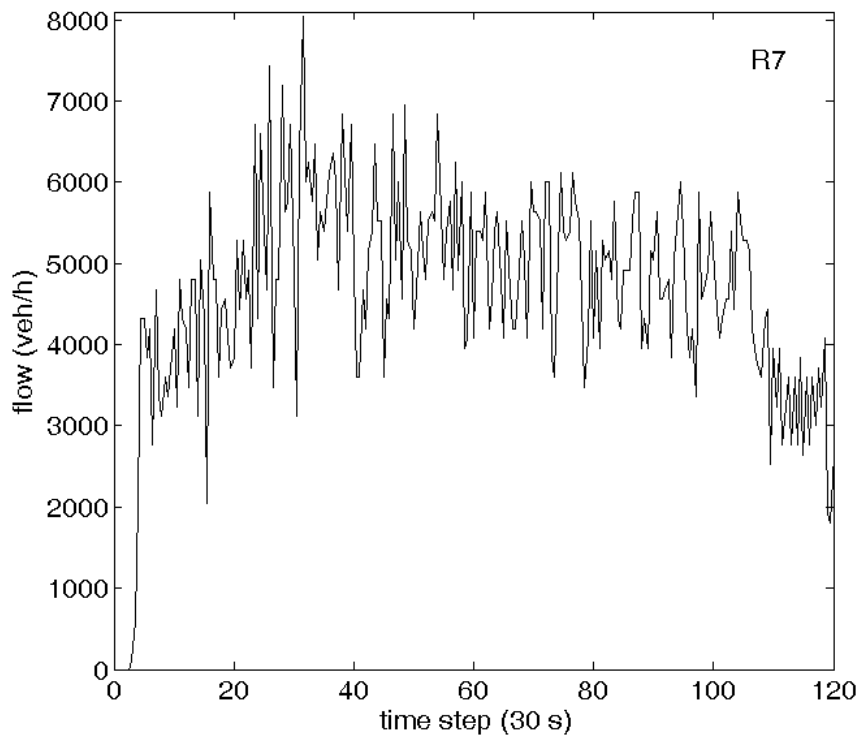


Figure 6-5: Merge area outflow in the no-control case.

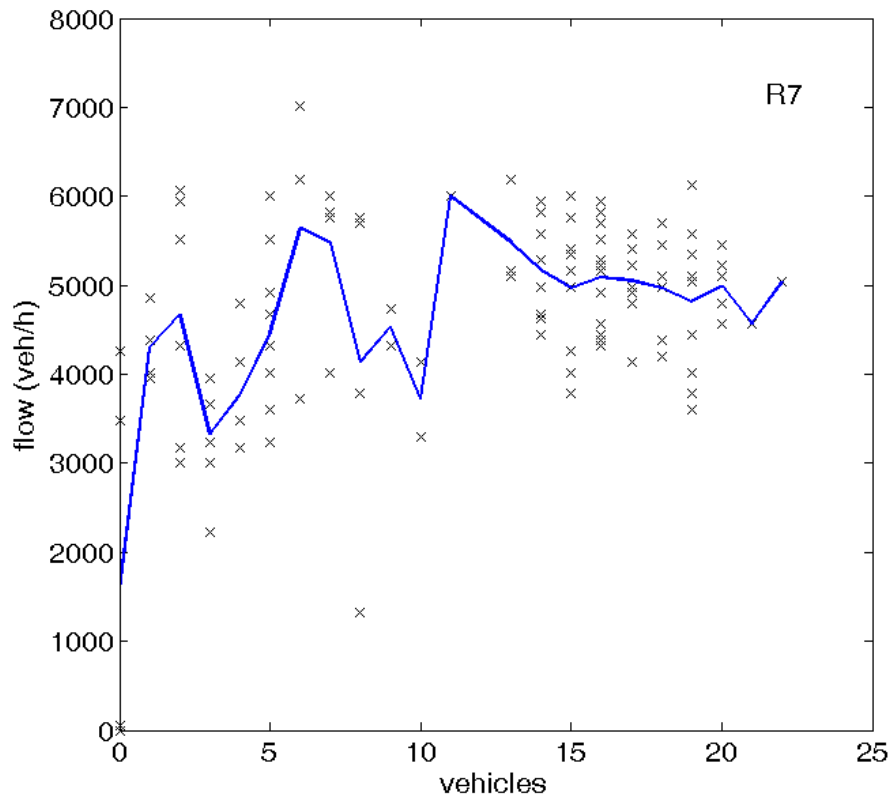


Figure 6-6: Outflow versus number of vehicles N in the no-control case.

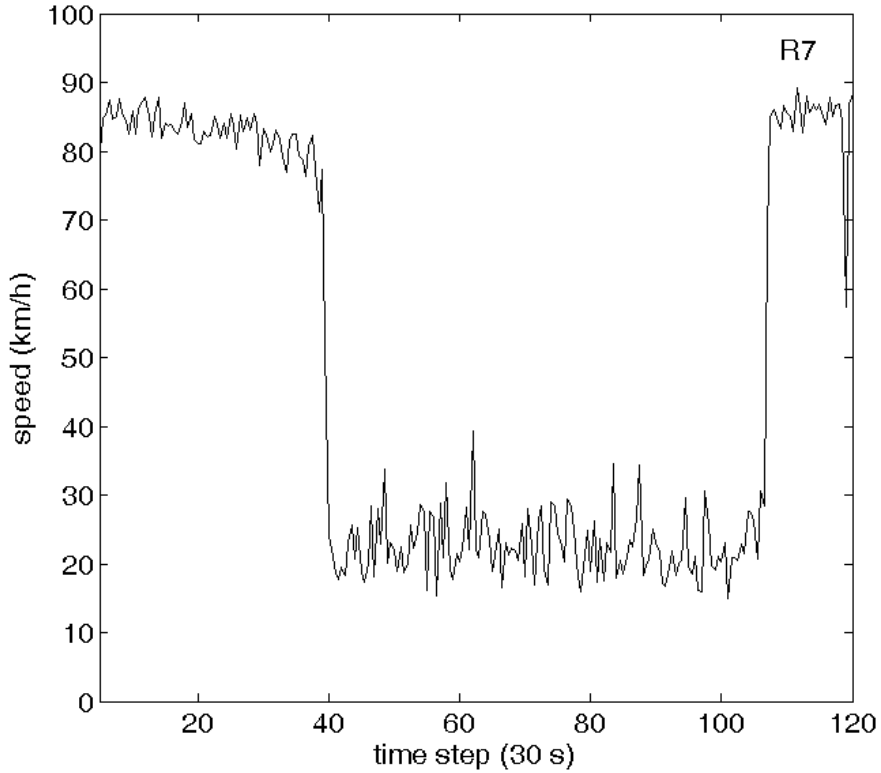


Figure 6-7: Speed at the merge entrance in the no-control case.

6.2 Control strategy PI-ALINEA

When merging traffic control is applied, the maximum admissible flow $q_{\max} = 6000$ veh/h is ordered by the regulator for as long as the number of vehicles N in the merge area is lower than the set value \hat{N} in PI-ALINEA'S equation (3-4). As the demand increases, N increases as well, and when $N(k)$ approaches \hat{N} , the controller starts its actual operation aiming at maintaining $N(k)$ close to \hat{N} . At this time queue is formed upstream of the traffic lights (since the arriving demand is higher than the work zone capacity) which propagates backwards, but without reaching the entrance of the simulated system (see Figure 6-8 and Figure 6-9).

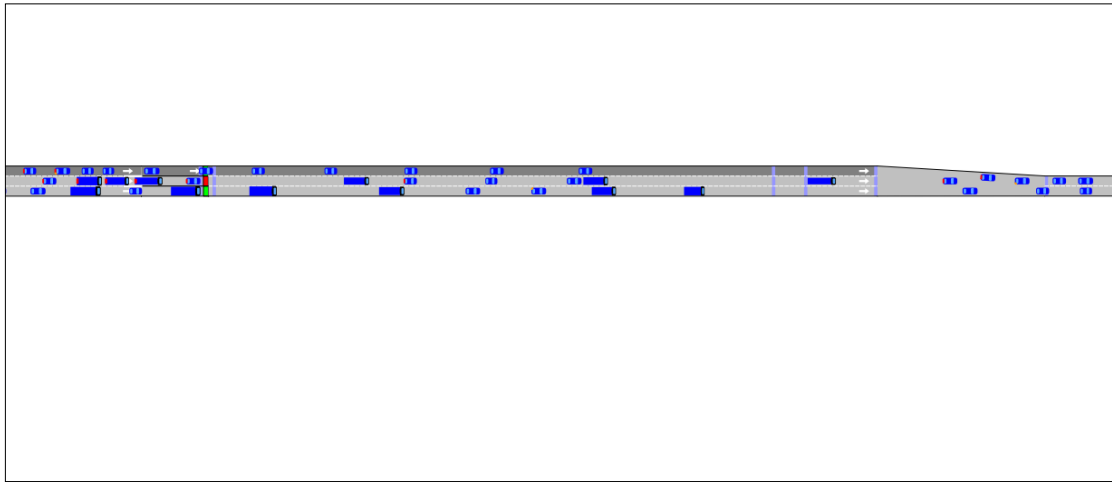


Figure 6-8: Control case, 37th minute of the simulation.

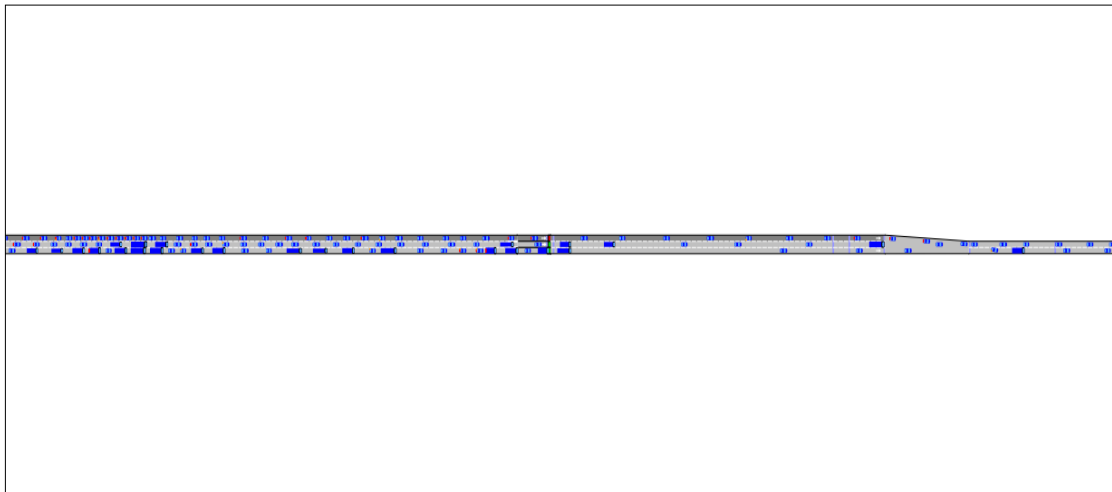


Figure 6-9: Control case, 40th minute of the simulation.

As it has been pointed out earlier, the main goal of merging traffic control is the maximization of the outflow from the merge area and the average vehicle delay minimization. Outflow maximization is enabled by determining an appropriate value for \hat{N} in equation (3-4). In a field investigation, this may be achieved by gradually incrementing \hat{N} and looking at the measured outflow, until a maximum throughput

is obtained. In the current research, the investigation of the \hat{N} -value is carried out through a series of simulation experiments with different (integer) \hat{N} -values within the range $\hat{N} \in [6, 20]$ veh. For each investigated \hat{N} value the AVD of 10 replications is obtained. As mentioned earlier, the values of the regulator parameters K_P and K_I are set equal to 150 h^{-1} and 6 h^{-1} , respectively. Figure 6-10 displays, for every investigated \hat{N} value, the corresponding AVD values for the 10 replications as well as the mean, minimum and maximum AVD of all replications. The mean, minimum and maximum AVD values of the 10 replications of the no-control case are also displayed on the same figure for comparison. According to the displayed results the mean AVD value is minimized in the range of $\hat{N} \in [9, 14]$ veh and particularly for \hat{N} equal to 11 veh it takes the lowest value, which corresponds to the critical value mentioned earlier. When \hat{N} is small, e.g. 6 vehicles, the mean AVD value is high because the corresponding outflow is less than the motorway capacity flow (the bottleneck starves for flow). When \hat{N} is big e.g., 18-20 vehicles, the mean AVD value is also high, but in this case due to the formed congestion in the merge area. It is also noteworthy that the mean AVD for all \hat{N} is significantly lower than the corresponding value of the no-control scenario. Particularly, for $\hat{N} = 11$ veh the resulted average improvement compared to the no-control case (see Table 6-1) is of 63 %, which is a significant achievement. Additionally, for this critical value the variation between the individual AVD values of the 10 replications is quite low.

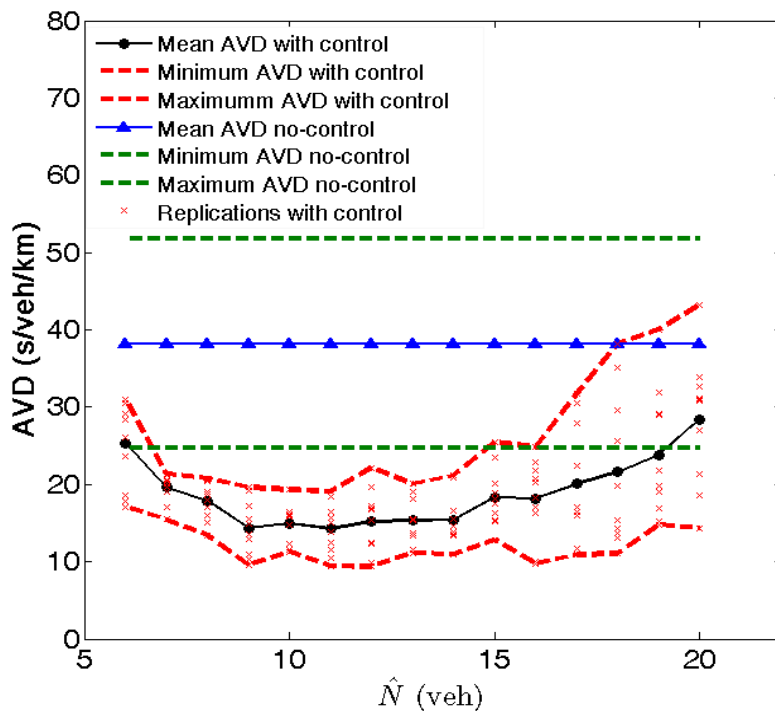


Figure 6-10: Average vehicle delay versus \hat{N} -values with and without control.

In the following paragraphs the obtained results for the control scenario are presented. The utilized regulator parameter values are $K_P = 150 \text{ h}^{-1}$, $K_I = 6 \text{ h}^{-1}$ and $\hat{N} = 11 \text{ veh}$. Table 6-2 displays the simulated results of the 10 replications as well as the corresponding mean, minimum and maximum AVD values.

Table 6-2: Simulation results for $\hat{N} = 11 \text{ veh}$.

Replication	Delay Time (s/veh/km)
1	12.43
2	19.11
3	15.70
4	16.51
5	9.44
6	13.83
7	11.58
8	15.01
9	18.45
10	10.41
Average Value	14.25
Minimum Value	9.44
Maximum Value	19.11

Figure 6-11 and Figure 6-12 display the number of vehicles in the merge area and the merge area outflow q_{out} , respectively, for replication 6 (R6) with $\hat{N} = 11 \text{ veh}$ and $AVD = 13.83 \text{ s/veh/km}$, which is closest to the mean AVD value of the corresponding 10 replications (Table 6-2). The number of vehicles in the merge area is maintained around the set-point $\hat{N} = 11 \text{ veh}$ (red dashed line in the figure) during the peak period. The observed spikes are due to stochastic arrivals, but also due to some occasional vehicle merging conflicts that may occur and lead to vehicle decelerations in the merge area; the appropriate reaction of the regulator in such cases, guarantees that the number of vehicles in the merge area remains around the set-point on average. The outflow q_{out} , as displayed in Figure 6-12, maintains its average value around 6000 veh/h during the peak period (between $t = 30 \text{ min}$ and $t = 60 \text{ min}$) and beyond the peak period for some 20 minutes because of the queued vehicles at the traffic lights. Figure 6-13 displays the merge area outflow versus the number of vehicles as well as the corresponding average flow values for every number of vehicles (blue line). For readability, the time step of the displayed measurements is equal to 1 min. Compared to the no-control case it can be observed that, despite some departures to higher N -values due to occasional merging conflicts, the feedback regulator actions brings traffic back to uncongested conditions so that no persisting congestion occurs in the merge area and the outflow q_{out} remains at a high level, in average. The improvement of the traffic conditions

can be also observed in Figure 6-14 where the mean vehicle speed upstream of the merge area is significantly increased during the peak hours to 70 km/h, except for the occasional departures to lower values due to corresponding merging conflicts.

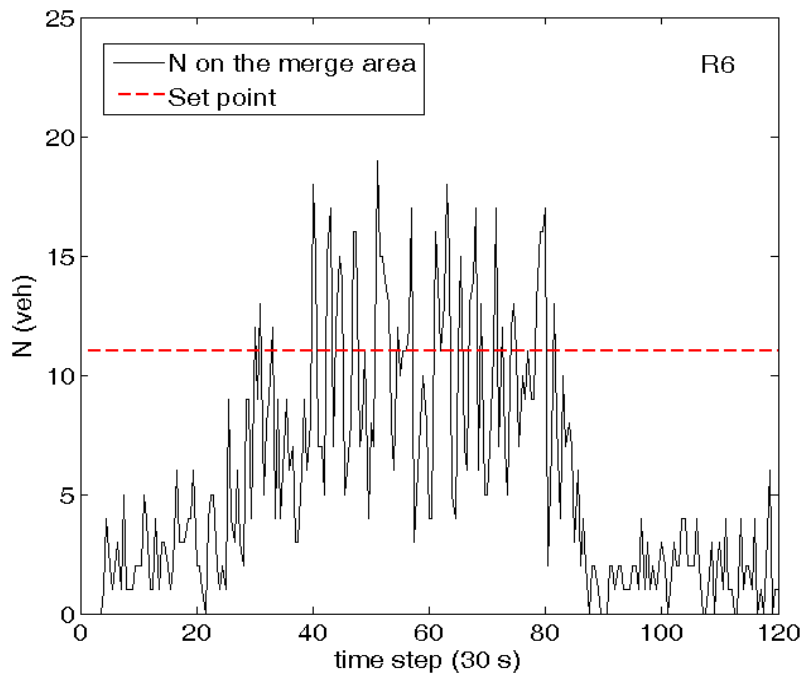


Figure 6-11: Number of vehicles in the merge area with control.

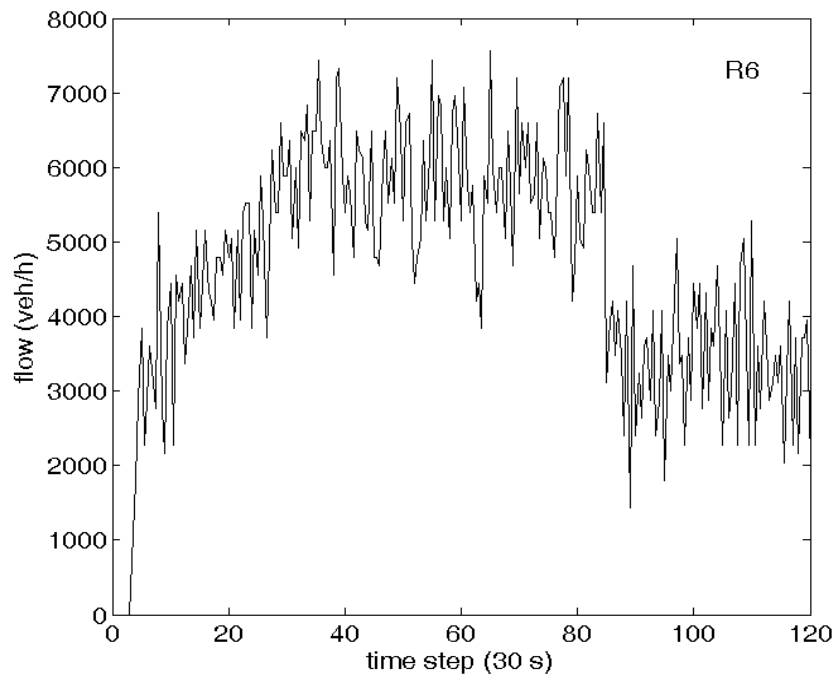


Figure 6-12: Merge area outflow with control.

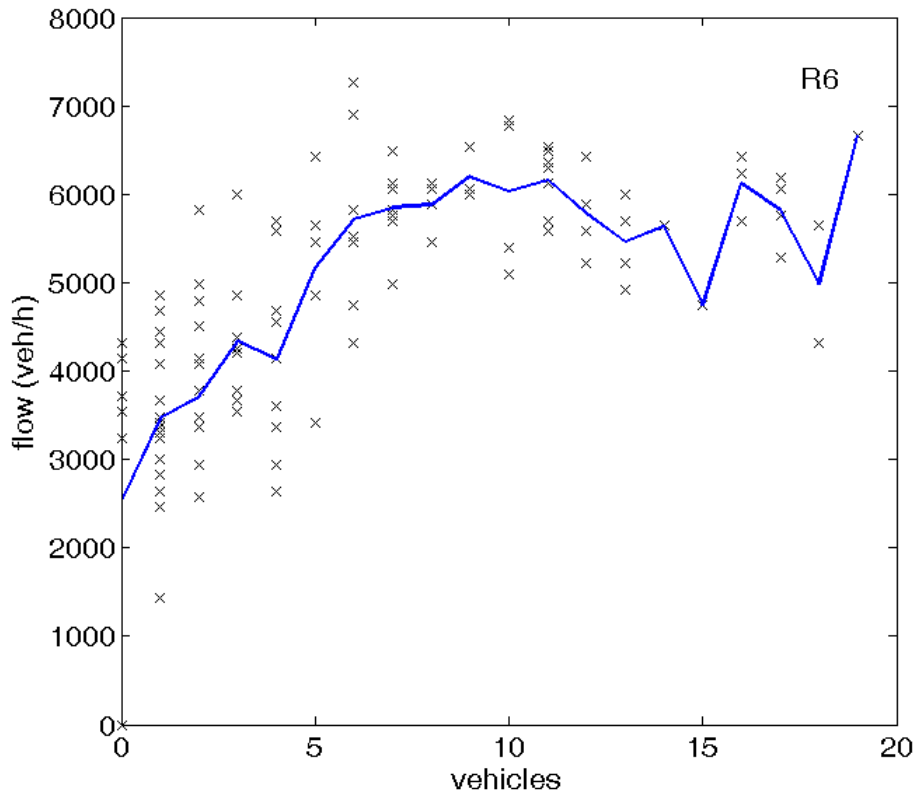


Figure 6-13: Outflow versus number of vehicles N in the control case.

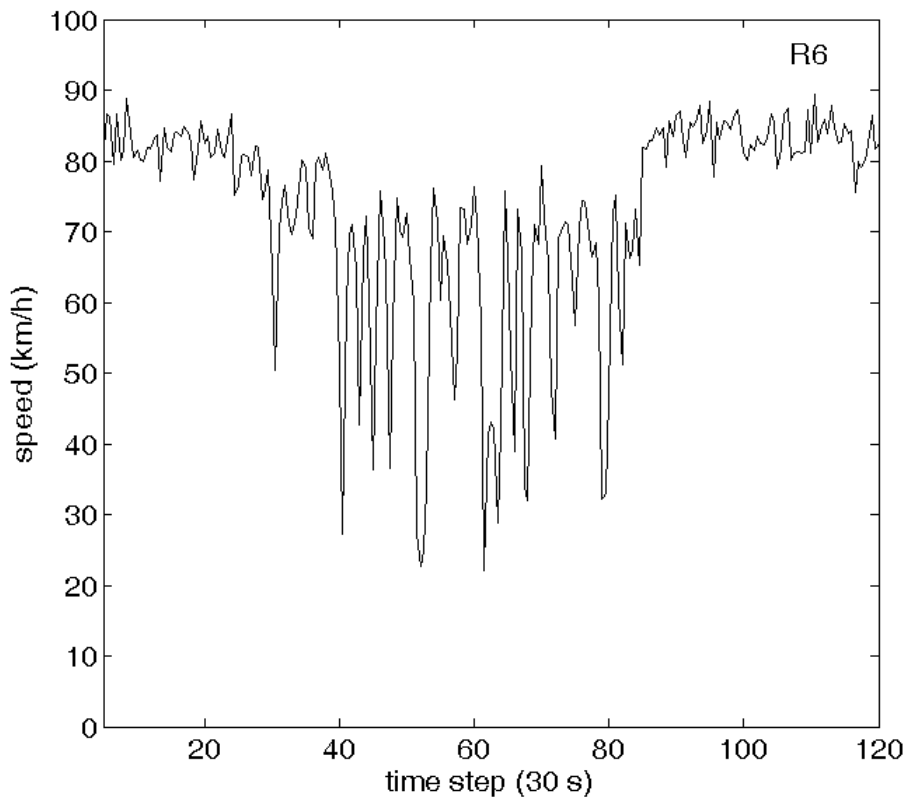


Figure 6-14: Speed upstream of the merge area with control.

6.3 Investigation of the position of the traffic lights

This section addresses the main objective of this research which is the investigation of the appropriate traffic lights position, when control is applied. The regulator parameter values that were specified in the previous section are $K_p = 150 \text{ h}^{-1}$, $K_i = 6 \text{ h}^{-1}$ and $\hat{N} = 11 \text{ veh}$ and are also utilized here.

The location of the traffic lights should be sufficiently upstream of the merge area in order to allow for the vehicles to accelerate and pass through the merge area efficiently, i.e. without major decelerations that give rise to the capacity drop observed in the no-control case. Considering a range of possible distances from 30 up to 400 m, 10 replications were simulated for each of them. The obtained mean AVD value as well as the acquired vehicle speed when approaching the merge area (save the occasional drops due to short-lasting merging conflicts) are the main evaluation criteria for the determination of the optimum position of the traffic lights. Figure 6-15 depicts, for every investigated traffic lights position, the resulting AVD values for the 10 replications, as well as the mean, minimum and maximum AVD for all replications. The trajectories of the mean, minimum and maximum AVD values for the 10 replications of the no-control case are also displayed on the same figure for comparison. The other important factor that is also evaluated is the average speed that vehicles have when approaching the merge area. Figure 6-16 displays the trajectories of the speed measurements collected upstream of the merge area, detector 4 in Figure 5-2, only for selected traffic lights positions, for readability.

As can be seen in Figure 6-15, the mean average vehicle delay is low and virtually constant when the traffic lights are located 150 m upstream of the merge area or more. In contrast, when traffic lights are placed very close to the merge area, higher AVD values are seen to result.

According to Figure 6-15 when the traffic lights are placed very close to the merge area, e.g. at 30 m or 50 m, vehicles do not have sufficient time to accelerate and indeed it can be observed that the mean speed value during the peak period is quite low, i.e. around 45 km/h. For a distance equal to 100 m, the merging vehicle speed starts increasing and reaches 60 km/h in average. For the traffic lights position of 200 m upstream of the merge area, the achieved merging vehicle speed has increased to a mean value around 70 km/h. For longer distances, e.g. 400 m, the speed is even more increased to around 80 km/h. The observed occasional speed drops during the maximum demand period, especially for long distances, are due to temporal sharp vehicle conflicts. Apparently, distances less than 150 m are not appropriate, and, particularly for distances less than 50 m, the system performance comes closer to the no-control case, because the capacity drop is only partially avoided. For distances more than 200 m, there is no further improvement, since the critical merging speed has been reached. Thus, 200 m is the most appropriate distance, as it

is preferable to have the traffic lights closer to the merge area. Table 6-3 displays the mean speed for every investigated traffic lights position, for each simulation run.

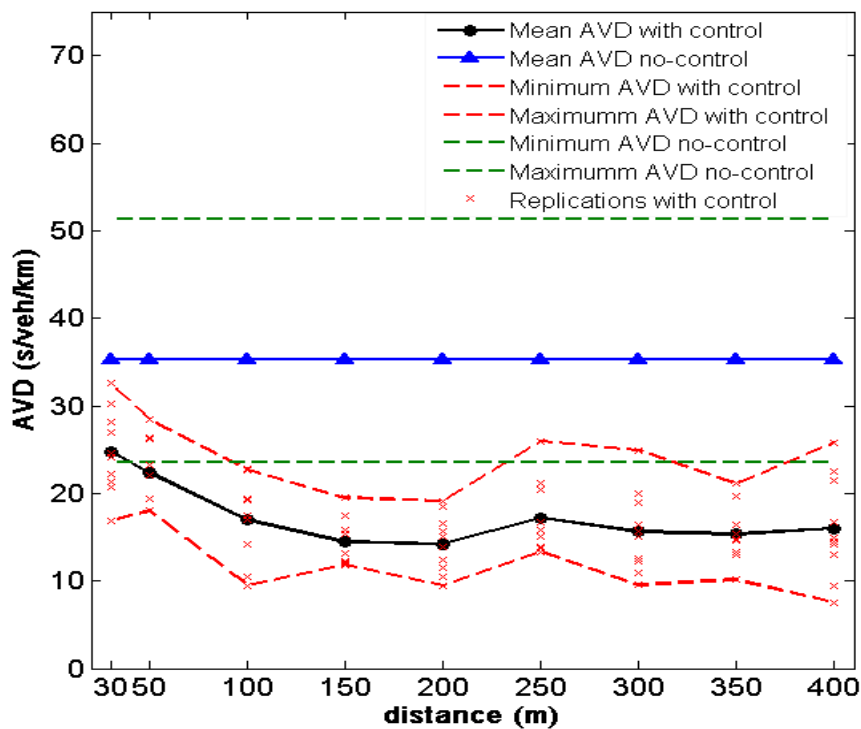


Figure 6-15: Average vehicle delay versus different traffic lights positions.

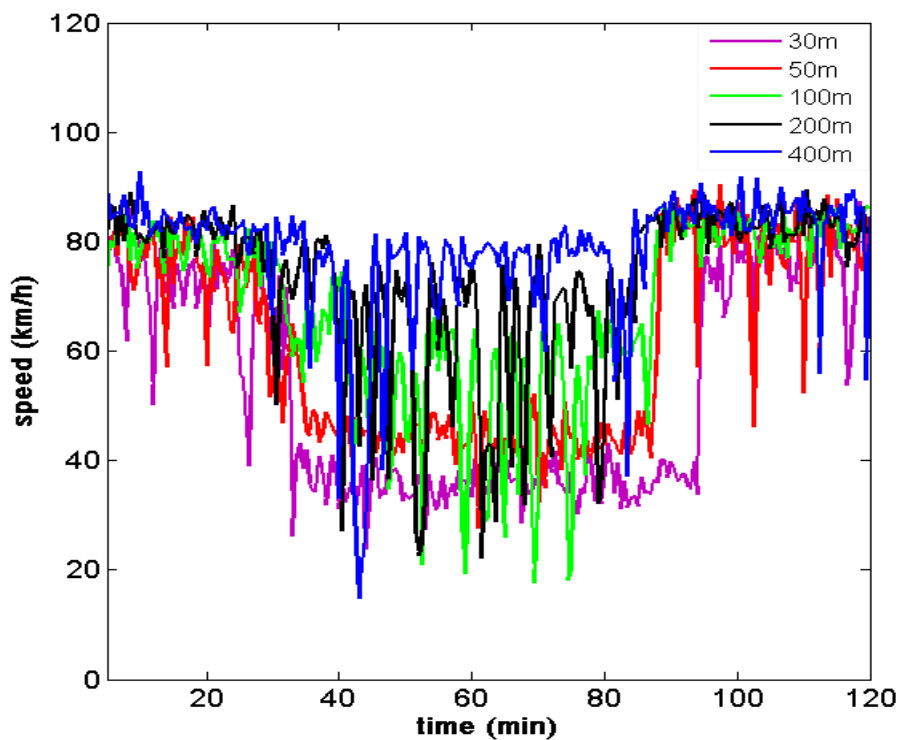


Figure 6-16: Speed versus different traffic lights positions.

Table 6-3: Speed measurements for the investigated traffic lights positions.

Repl.	30 m <i>Mean speed (km/h)</i>	50 m <i>Mean speed (km/h)</i>	100 m <i>Mean speed (km/h)</i>	150 m <i>Mean speed (km/h)</i>	200 m <i>Mean speed (km/h)</i>	250 m <i>Mean speed (km/h)</i>	300 m <i>Mean speed (km/h)</i>	350 m <i>Mean speed (km/h)</i>	400 m <i>Mean speed (km/h)</i>
1	54.68	60.99	64.21	72.06	73.93	71.45	74.38	76.06	74.42
2	51.11	58.18	64.94	73.12	72.82	70.86	75.51	75.44	71.79
3	52.54	60.80	65.44	70.75	74.35	73.41	76.34	74.05	73.15
4	54.33	59.52	69.40	72.70	76.38	75.31	75.72	78.02	77.24
5	53.59	59.12	67.99	71.46	76.33	73.78	77.65	76.02	74.74
6	53.33	59.25	68.60	71.18	72.67	74.64	76.48	78.24	76.52
7	54.15	60.90	67.74	72.74	75.23	78.02	76.55	75.64	77.81
8	54.85	58.84	67.03	71.35	72.37	71.05	75.12	76.27	78.77
9	52.42	59.24	68.38	72.10	71.81	74.57	76.18	73.64	77.63
10	55.18	60.11	70.75	73.06	76.83	73.49	68.03	77.78	77.13
Avg.	53.62	59.69	67.45	72.05	74.27	73.66	75.20	76.12	75.92

Compared to the corresponding no-control scenario (see Table 6-1), the implementation of the control concept accomplishes to improve the system performance significantly. For the position of the traffic lights 200 m upstream of the merge area, the mean AVD is notably improved to some 63 %, while the mean speed is 70 km/h on average (34 % improvement). Additionally, the merge area throughput is increased to 6000 veh/h during the peak period (20 % improvement compared to the no-control case).

7 Application of AFT to the merging control strategy

7.1 The Adaptive Fine-Tuning (AFT) Algorithm

Despite the continuous advances in the fields of control and computing, the design and deployment of an efficient Large-scale Nonlinear Traffic Control System (LNTCS) remains a significant objective, mainly because of the involved complexity and the strong nonlinearities. The ultimate performance of a designed or operational LNTCS (e.g. urban signal control, or ramp metering, or Variable Speed Limit (VSL) control) depends on two main factors: (a) the exogenous influences, e.g. demand, weather conditions, incidents, and (b) the values of some design parameters included in the LNTCS.

As a matter of fact, when a new control algorithm is implemented (or an operational but “aged” control algorithm needs to be updated), there is a period of, sometimes tedious and time-consuming, fine-tuning activity that is needed in order to elevate the control algorithm to its best achievable performance. Fine-tuning concerns the selection of appropriate (or even optimal) values for a number of design parameters included in the control strategy. Typically, this fine-tuning procedure is conducted manually, via trial-and-error, relying on expertise and human judgment and without the use of a systematic approach.

Currently, a considerable amount of human effort and time is spent for calibration of operational LNTCSs. Minor changes in the transport system infrastructure (e.g. installing a new Variable Message Sign (VMS) in a motorway network, modifying the traffic light signal phasing at an urban junction, deploying a new bus in a public transport system or a new Automated Guided Vehicle (AGV) in a seaport container terminal) may require the involvement of significant human effort and time in order to re-adjust and re-program the LNTCS decision making mechanisms.

Moreover, the continuous medium- and long-term variations of the overall transport system dynamics (e.g. due to changes of traffic demand or number of passengers using the particular transport system) call for a frequent or even continuous maintenance of LNTCSs, which – if done properly – it is extremely costly. In many cases, the result is that system maintenance is neglected and the system performance deteriorates year after year.

As presented in chapters 5 and 6, the calibration of the regulator parameter values was conducted manually via trial-and-error. However, this manual optimization practice may be quite tedious and time-consuming, especially for very complex problems, and requires expertise judgment in order to select the appropriate values of the parameters included in the control strategy. Recently, a learning/adaptive

algorithm called AFT (Adaptive Fine-Tuning) was proposed (Kouvelas, 2011; Kouvelas et al., 2011) to enable automatic fine-tuning of traffic control systems (TCS), so as to reach the best measurable performance that is achievable with the applied control strategy. In this chapter the automatic fine-tuning method is employed for the motorway work-zone merging control concept in order to automatically fine-tune the regulator parameters of the PI-ALINEA control strategy. In the following paragraphs a brief description of the AFT algorithm is presented. A detailed presentation of the AFT algorithm and its applications can be found in Kouvelas, 2011. The basic functioning procedure of the AFT algorithm may be summarized as follows (Figure 7-1):

- ❖ The traffic flow process (e.g. motorway road network) is controlled in real time by a control strategy which includes a number of parameters to fine-tune.
- ❖ At the end of appropriately defined periods (e.g. at the end of each day in field applications), the AFT algorithm receives the value of real (measured) performance index (e.g. average vehicle delay, etc.), as well as some aggregated values of the most significant external factors (e.g. demand). Note that the performance index is a function of the external factors and the tunable parameters to be adjusted.
- ❖ Using the measured quantities (the number of which increases iteration by iteration), the AFT algorithm calculates new tunable parameter values to be applied at the next period (e.g. the next day) in an attempt to improve the system performance.
- ❖ This (iterative) procedure is continued over many periods (e.g. days) until a maximum in performance is reached; then, the AFT algorithm may remain active for continuous adaptation or can be switched off and re-activated at a later stage (e.g. after few months).

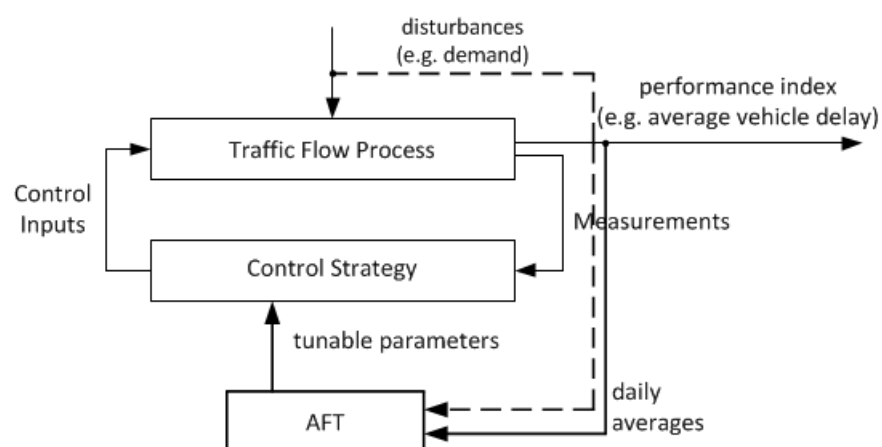


Figure 7-1: Working principle of AFT for automatic calibration of LNTCSs.

In the current study, one AFT iteration corresponds to the duration of the demand scenario (2 hours) as well as no disturbances are considered.

The original algorithm employs a polynomial-like approximator (similar to a neural network) that approximates, based exclusively on available real measurements, the unknown nonlinear performance function of the problem. For this application, a polynomial approximator as well as a Support Vector Machine (SVM) model (see Burges et al., 1998) are used. This methodology was recently used in (Giannakis, et al., 2011) in order to fine-tune the parameters of a building's controller.

The AFT algorithm is started with some initial values for the parameters to be tuned. When using an SVM approximator, the algorithm converges faster to a closer local minimum of the performance function and remains there; while the original AFT may feature more significant "jumps" in the parameter space, with correspondingly stronger fluctuations of the performance function. In order to use SVM, a sufficient initial set of training data is needed to be available for fitting. Therefore, the original AFT (using the polynomial approximator) is applied for the first 10 iterations, before switching to the SVM usage. In particular, for the first 10 iterations, AFT explores a wide region of alternative sets of parameters; following which the SVM is used and the algorithm converges to a close local minimum without exploring other feasible regions.

Several simulation experiments are conducted in this study so as to evaluate the efficiency of the AFT algorithm for the problem of optimizing the regulator parameters. In order to assess the overall system performance, the fine-tuning experiments are conducted based on the minimization of two different evaluation criteria. The first is the average vehicle delay (AVD) of the traffic network during the whole simulation period. Moreover, for this case two different types of experiments are examined: (1) when all the regulator parameters K_p , K_I and \hat{N} are selected for fine-tuning by the AFT algorithm, and (2) when only two of the parameters K_p and K_I are fine-tuned for a given set point value, \hat{N} . An alternative objective criterion for the problem addressed in this research is the standard deviation of the regulation error derived from the regulator equation (Equation 3.16) over the "peak hours period" of the demand scenario.

All the aforementioned simulation experiments are conducted using AIMSUN simulator and the obtained simulation results are presented in the following sections. The obtained simulation results from the automatic fine-tuning procedure are compared to the base-case, where the regulator parameters were derived manually.

7.2 Application of AFT with AVD as the objective criterion

This section presents the application results of the AFT algorithm when considering the average vehicle delay (AVD) as the objective criterion to be minimized. Because of the nonconvexity of the problem, it is not possible to find the global minimum of the problem and the algorithm converges to different local minima depending on the given starting points. For this reason, the AFT algorithm is applied for various control scenarios with different initial values of the tunable parameters, so as to investigate the behavior of the algorithm under different conditions.

Before applying the AFT algorithm, each hypothetical control scenario is implemented to the work-zone concept and the simulation results of 10 different replications are collected. Then, the AFT algorithm is applied for each control scenario and the derived set values after the algorithm's convergence are considered as new control scenarios to be implemented. In order to evaluate the performance of the algorithm, the simulation results from the implementation of the new control scenarios for 10 different replications (different seeds) are finally compared with the corresponding results delivered from the implementation of the initial control scenarios (before the use of the AFT algorithm). For each AFT run, 100 iterations (fine-tuning experiments) are simulated, consisting of the aforementioned 10 replications.

In this research, four hypothetical control scenarios are examined. In the first three, all the regulator parameters, K_p , K_I and \hat{N} are selected for fine-tuning by the AFT algorithm, for given initial set values. In the last control scenario, the tunable parameters are only K_p and K_I , while the set point \hat{N} is fixed.

In the following sections, the AFT algorithm results are presented as well as the corresponding results for each applied control scenario before and after the use of the AFT algorithm.

7.2.1 Control scenario 1

In the first experiment the AFT algorithm is applied for a control scenario with the initial values of the tunable parameters set as following: $K_p = 150 \text{ h}^{-1}$, $K_I = 6 \text{ h}^{-1}$ and $\hat{N} = 11 \text{ veh}$. These are the optimized parameters values derived via the trial-and-error method (Chapters 5 and 6), which means that these values are already considered as “good” starting values for the AFT algorithm. Figure 7-2 displays the AVD values trajectory delivered for three different runs of the AFT algorithm. The purpose of this experiment is to confirm whether the manually optimized values for the regulator parameters are indeed appropriate for the applied control strategy or if further improvement of the system's performance can be provided by an automatic fine-tuning procedure. Figures 7-3—7.5 display the trajectories of the corresponding runs for each tunable parameter of the system.

As it can be seen in Figure 7-2, some strong fluctuations are observed in the first 20 iterations, but during the rest fine-tuning period the AFT algorithm achieves to keep the AVD at low values. In the trajectories of the tunable parameters it is observed that in the first iterations the oscillations are strong as the AFT algorithm is learning the system's behavior by experimenting with different sets of parameters. However, after a few iterations the performance of the AFT algorithm is better and the convergence to a local minimum is clear. Particularly, for every AFT run the algorithm converges at the following values of the parameters: (1) for the first AFT run $K_p = 80.88 \text{ h}^{-1}$, $K_i = 2.95 \text{ h}^{-1}$ and $\hat{N} = 8.37 \text{ veh}$, (2) for the second AFT run $K_p = 160.42 \text{ h}^{-1}$, $K_i = 7.33 \text{ h}^{-1}$ and $\hat{N} = 12.6$, and for the third AFT run $K_p = 152.85 \text{ h}^{-1}$, $K_i = 5.25 \text{ h}^{-1}$ and $\hat{N} = 11.27$. The delivered set values are then applied to the work-zone control concept in order to compare the system performance before and after the use of the AFT algorithm.

In Table 7-1 the AVD values are displayed, for the case before the use of AFT and for the first AFT run, resulting from 10 simulation runs. It is noteworthy that for this experiment the use of the AFT algorithm efficiently fine-tunes the regulator parameters and leads to an additional improvement of the mean AVD value of about 8.63 %. The resulting mean AVD values (in s/veh/km) for the other two AFT runs are 13.95 and 14.99, respectively. Obviously, in the third AFT run the algorithm did not achieve to further improve the system's performance as it remained very close to the already "good" local minimum.

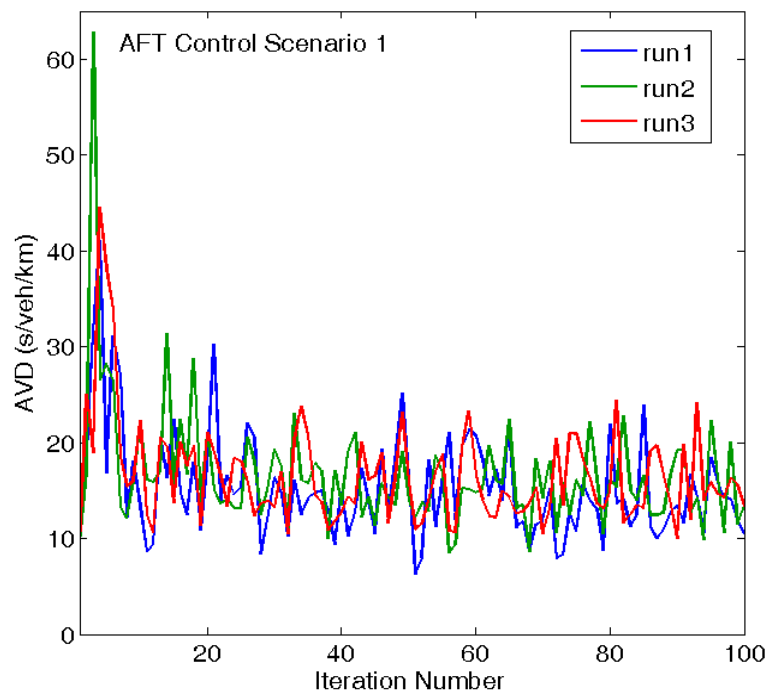


Figure 7-2: Average vehicle delay for control scenario 1.

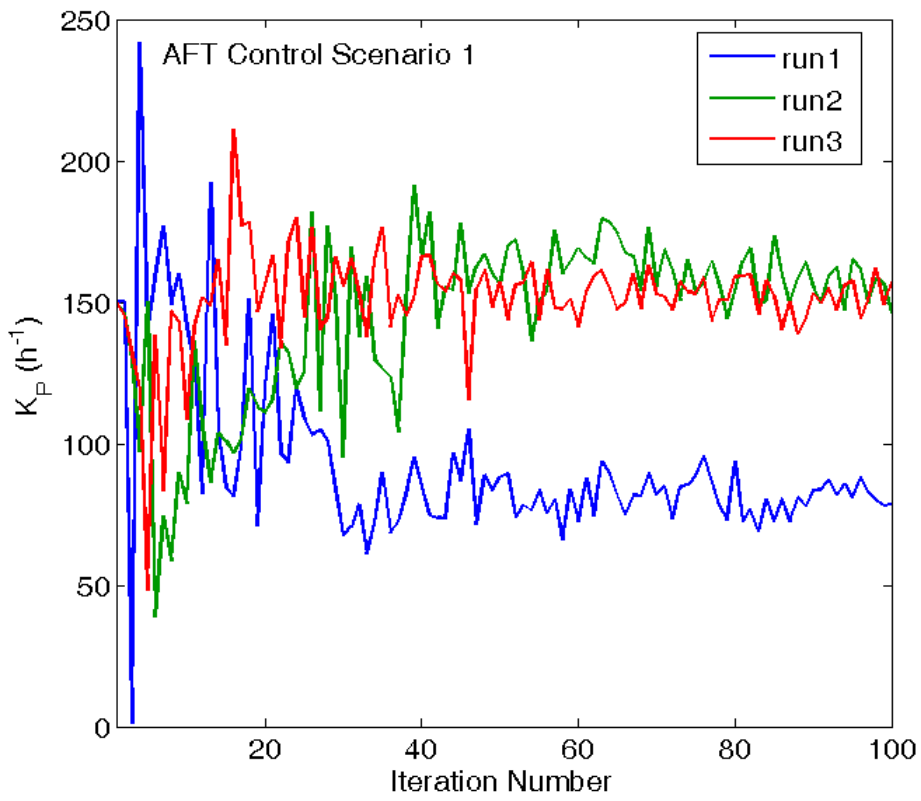


Figure 7-3: K_P parameter for control scenario 1 (1 AFT run).

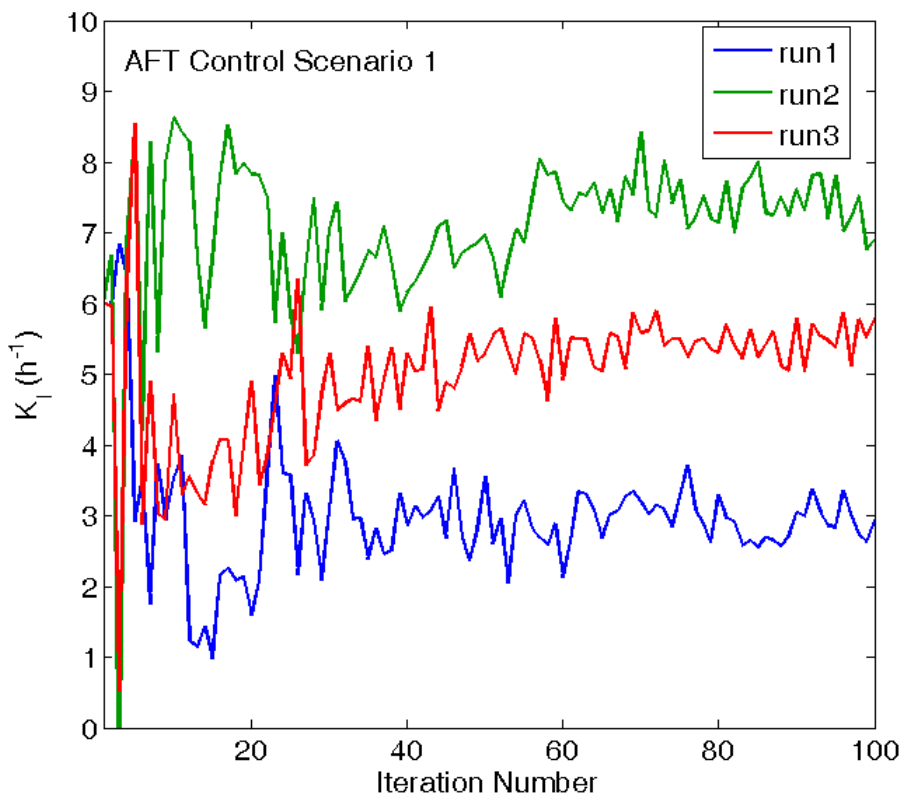


Figure 7-4: K_I parameter for control scenario 1 (1 AFT run).

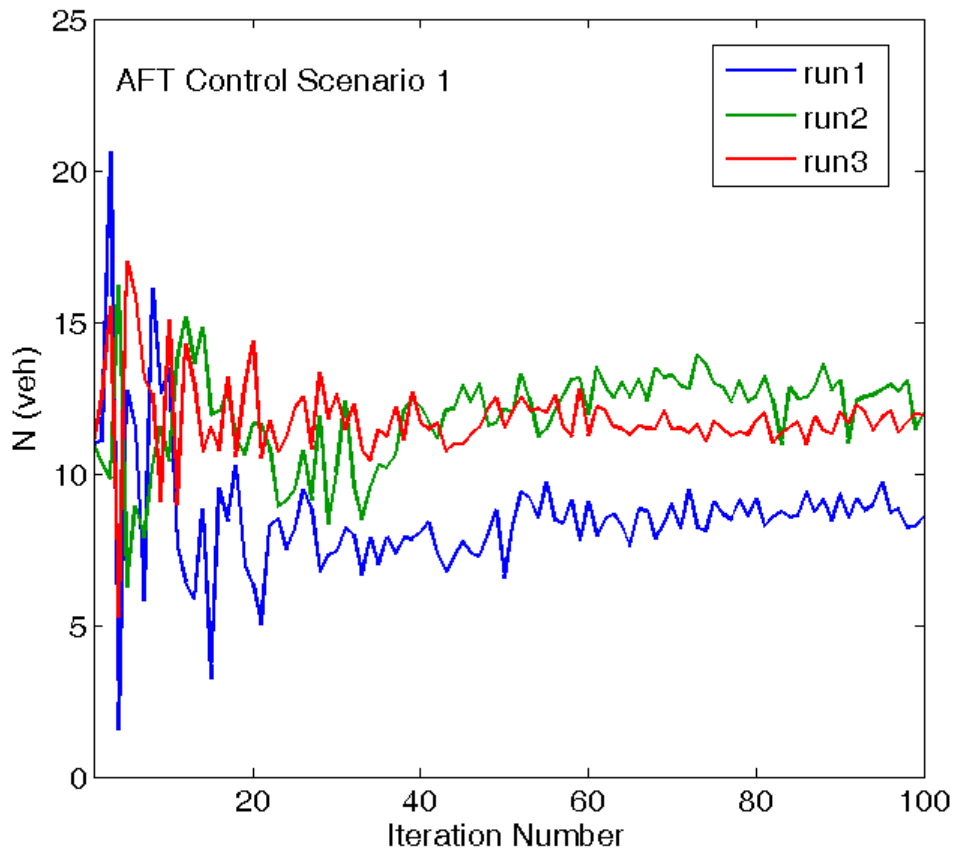


Figure 7-5: \hat{N} parameter for control scenario 1 (1 AFT run).

Table 7-1: Comparison of the average vehicle delay (AVD) with and without the application of AFT algorithm.

Replications	Before AFT	After AFT (run 1)
	$K_p = 150, K_I = 6, \hat{N} = 11$ AVD (s/veh/km)	$K_p = 80.88, K_I = 2.95, \hat{N} = 8.37$ AVD (s/veh/km)
R1	12.43	9.48
R2	19.11	13.35
R3	15.70	20.95
R4	16.51	9.41
R5	9.44	10.92
R6	13.83	18.83
R7	11.58	12.39
R8	15.01	8.87
R9	18.45	14.13
R10	10.41	11.87
Average Value	14.25	13.02
Minimum Value	9.44	8.87
Maximum Value	19.11	20.95

7.2.2 Control scenario 2

The initial values of the tunable parameters chosen for the second scenario are $K_p = 50 \text{ h}^{-1}$, $K_I = 10 \text{ h}^{-1}$ and $\hat{N} = 10 \text{ veh}$. This set of parameters is randomly

selected in order to investigate the algorithm’s behavior. Figures 7-5—7-8 present for two AFT runs the trajectories of the AVD values and of the tunable parameters during the fine-tuning process. In Figure 7-6 it is visible for the first AFT run (blue line) that the AVD values oscillate due to the search process of AFT algorithm, but finally AFT achieves to keep the mean AVD value low. On the other hand, AFT did not improve the system’s performance in the second run, as there is no significant change in the mean AVD value according to the figure. As observed in the trajectories of the tunable parameters in Figures 7-7—7-9, for the first AFT run, in the first iterations the fluctuations are quite strong but after a while the AFT algorithm converges to some values by efficiently fine-tuning the regulator parameters. According to these figures, the AFT algorithm converges to $K_P = 73.83 \text{ h}^{-1}$, $K_I = 4.53 \text{ h}^{-1}$ and $\hat{N} = 8.59 \text{ veh}$. In the second AFT run, the algorithm converges to $K_P = 49.99 \text{ h}^{-1}$, $K_I = 7.61 \text{ h}^{-1}$ and $\hat{N} = 8.82 \text{ veh}$. It is notable that these values are very close to the initial ones (before the use of AFT) and consequently the algorithm could not provide additional improvement as it remained in the same area.

Table 7-2 displays the resulting AVD values for 10 replications after applying the control scenario before the use of the AFT algorithm and the AVD values for the new control scenario after the system fine-tuning by AFT. The resulting mean AVD value (in s/veh/km) for the second AFT run is 20.37.

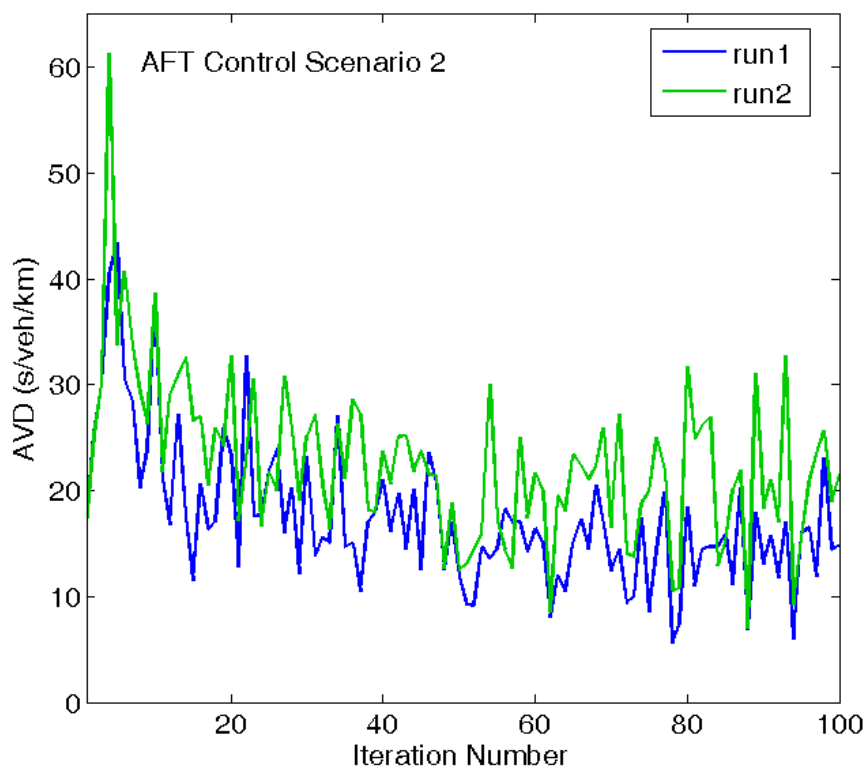


Figure 7-6: Average vehicle delay for control scenario 2.

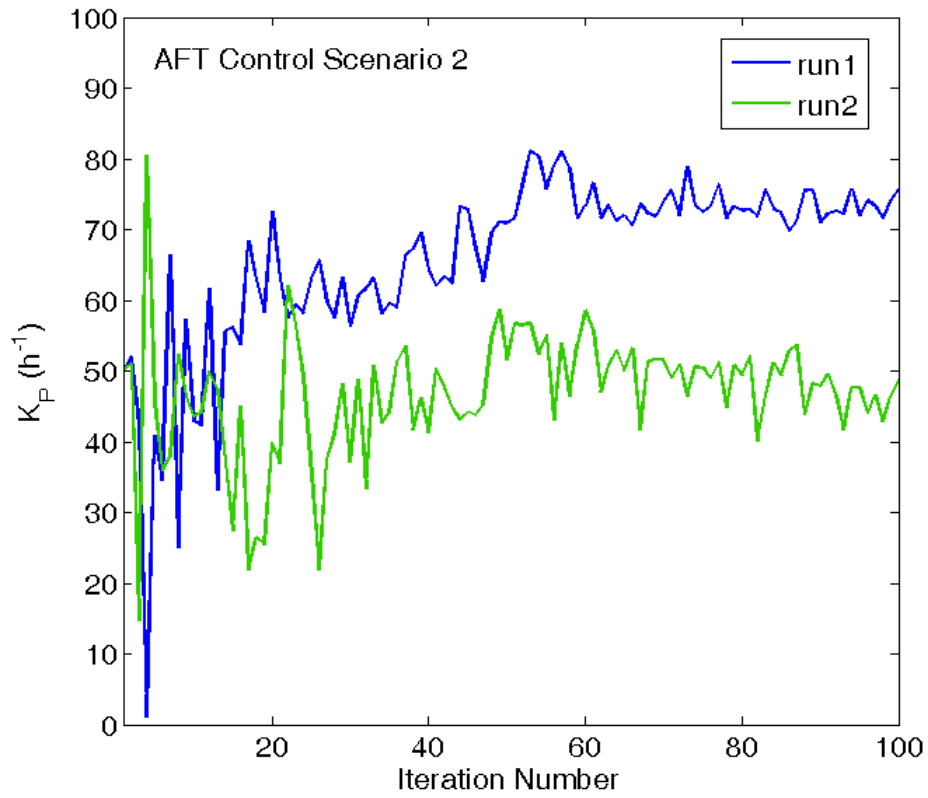


Figure 7-7: K_P parameter for control scenario 2 (1 AFT run).

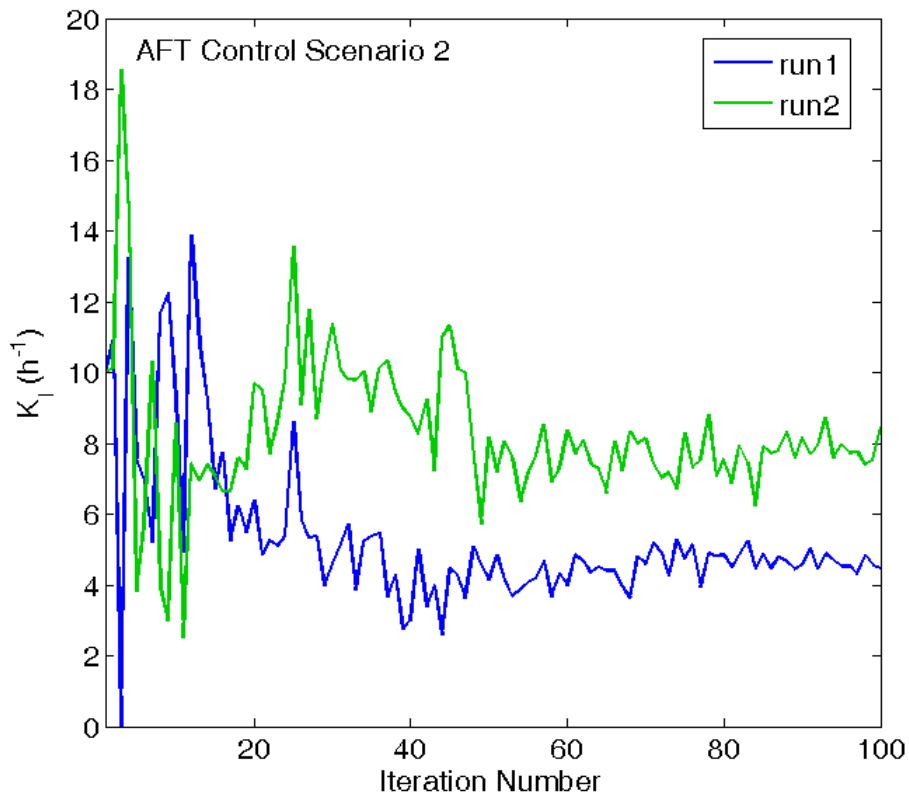


Figure 7-8: K_I parameter for control scenario 2.

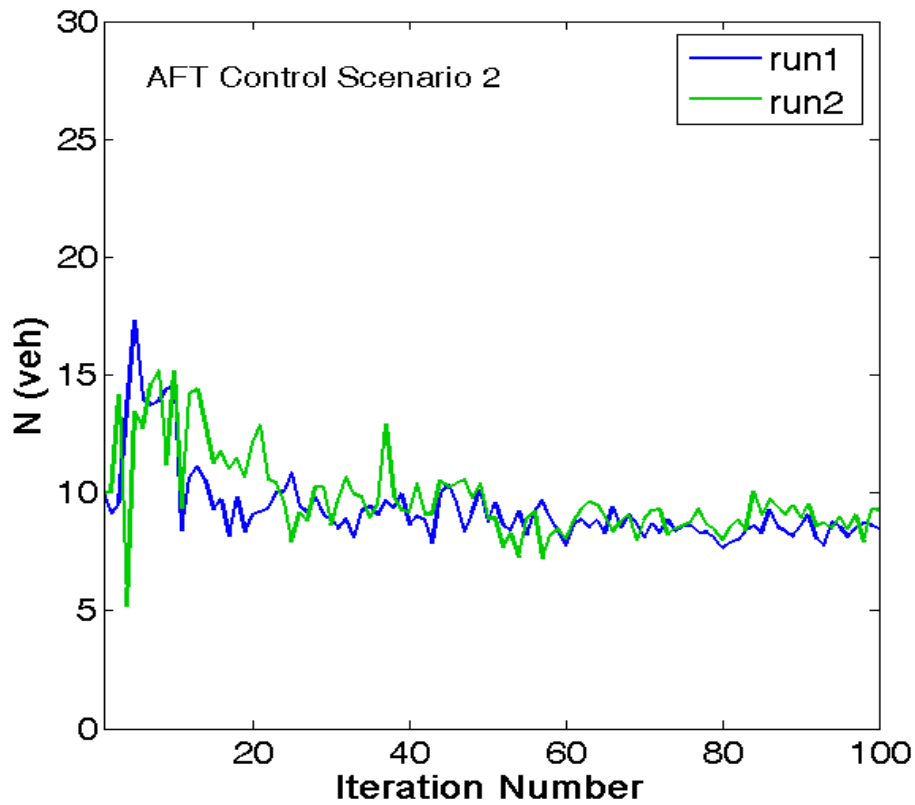


Figure 7-9: \hat{N} parameter for control scenario 2.

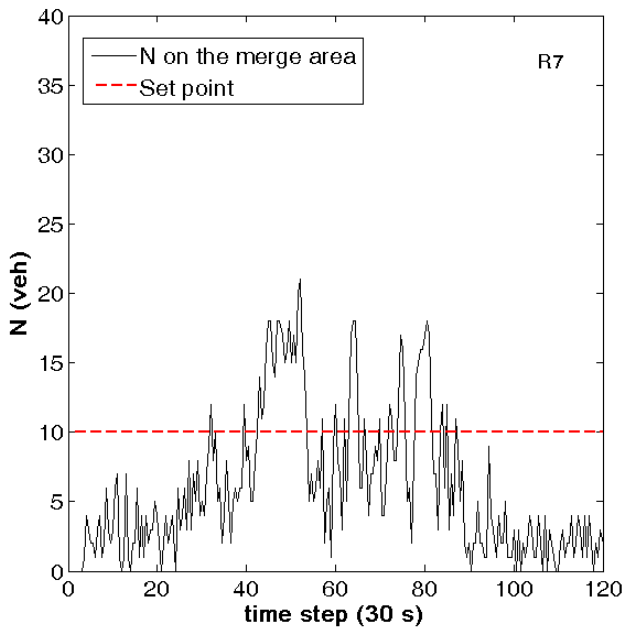
Table 7-2: Comparison of the average vehicle delay (AVD) with and without the application of AFT.

Replications	Before AFT	After AFT (run 1)
	$K_p = 50, K_I = 10, \hat{N} = 10$ AVD (s/veh/km)	$K_p = 73.83, K_I = 4.53, \hat{N} = 8.59$ AVD (s/veh/km)
R1	14.99	21.37
R2	26.94	18.25
R3	31.49	12.20
R4	35.29	11.41
R5	16.71	13.55
R6	15.86	13.53
R7	20.86	14.06
R8	14.98	11.78
R9	20.36	16.08
R10	15.56	8.70
Average Value	21.30	14.09
Minimum Value	14.98	8.70
Maximum Value	35.29	21.37

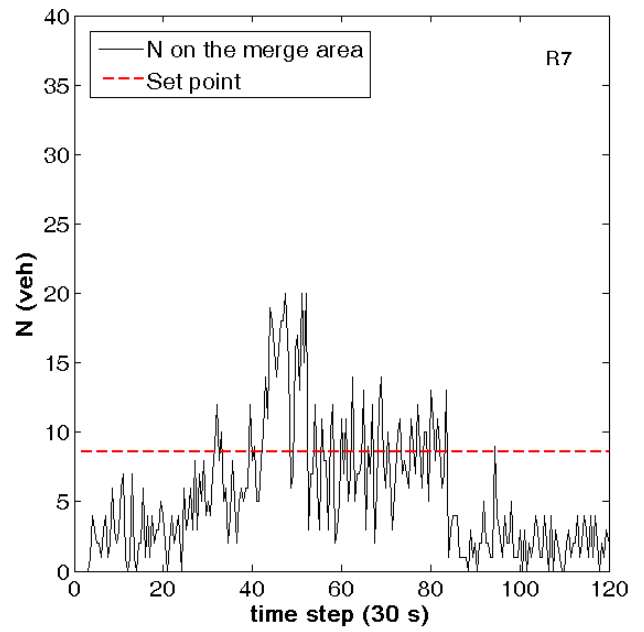
As seen in Table 7-2, the simulated results for the control scenario before the use of AFT algorithm indicate quite high AVD values with a mean AVD value around 21.30 s/veh/km. However, after the implementation of the new control scenario, the resulting AVD values are sufficiently low. The additional improvement of the mean AVD value is significantly high around 33.85 %, which is considered as a well-conducted system fine-tuning by the AFT algorithm. Moreover, according to the resulting mean AVD value after the use of AFT (Table 7-2) the performance of the control scenario is even slightly better than of the implemented control scenario after the manual fine-tuning of the regulator parameters (see Chapter 6.3, Table 6-2).

The improvement of the system's performance can be also clearly observed in the following figures, which present other measurements (e.g. outflow values, speed values etc.) for the control scenarios examined in this section. Particularly, Figures 7-10 (a) and 7-10 (b) present for one replication the number of vehicles in the merge area during the whole simulation horizon for the initial control scenario before the use of the AFT algorithm, as well as the corresponding values for the delivered control scenario after the use of AFT. It can be observed in Figure 7-10(b) that the number of vehicles in the merge area remains in average close to the set-point $\hat{N} = 8.59$ veh (red line in the figure) for a longer time period compared to the corresponding diagram before the use of AFT with the set-point $\hat{N} = 10$ veh. Figures 7-11(a) and 7-11(b) display the merge area outflow before and after the use of AFT algorithm. Comparing the two figures it can be observed that after the use of AFT the average outflow is increased. Figures 7-12 (a) and 7-12 (b) display the outflow versus the number of vehicles N in the merge area for the aforementioned control scenarios. It can be clearly observed in Figure 7-11b that compared to the initial control scenario the traffic conditions are improved and no congestion occurs.

Finally, in Figures 7-13 (a) and 7-13 (b) the trajectories of speed measurements taken upstream of the merge area are presented (detector 4 in Figure 5-2). After the use of AFT the average vehicle speed is increased to 75 km/h in average. Additionally, in the trajectory of Figure 7-13 (b) (after the use of AFT) the oscillations are reduced compared to the speed trajectory of Figure 7-13 (a) (before the use of AFT). Actually, that means that the time period of congestion during the simulation is reduced and the vehicles decelerations are limited. The corresponding results of the other replications are similar to those described above.

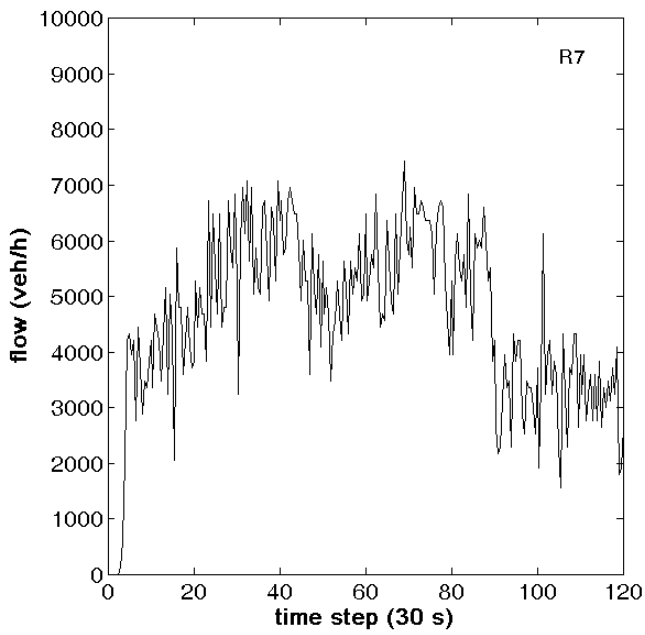


(a)

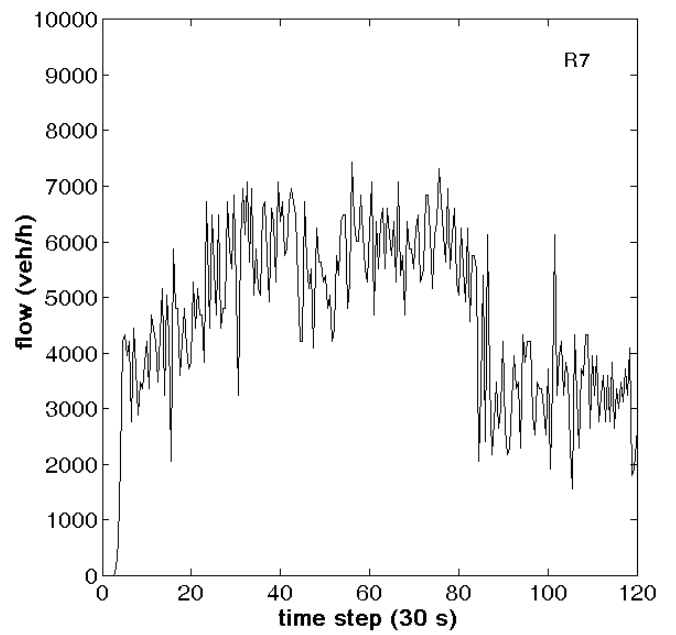


(b)

Figure 7-10: Number of vehicles in the merge area (a) before the use of AFT and (b) after the use of AFT.

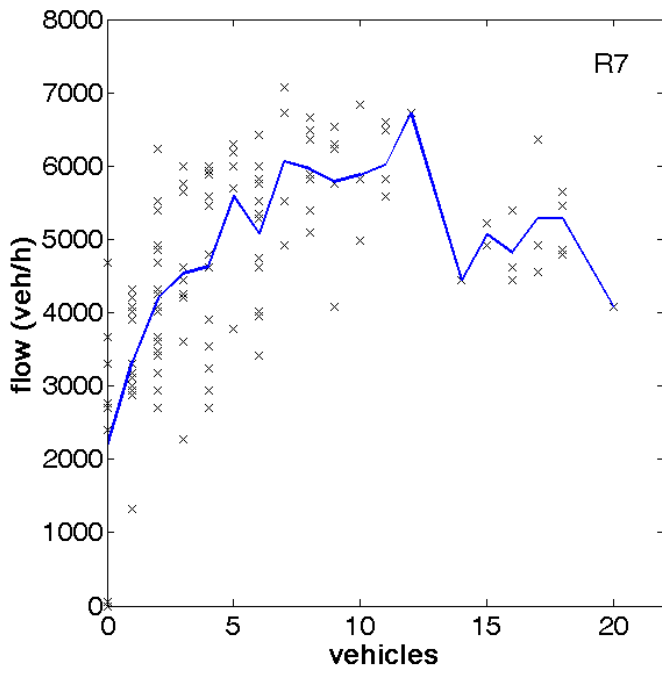


(a)

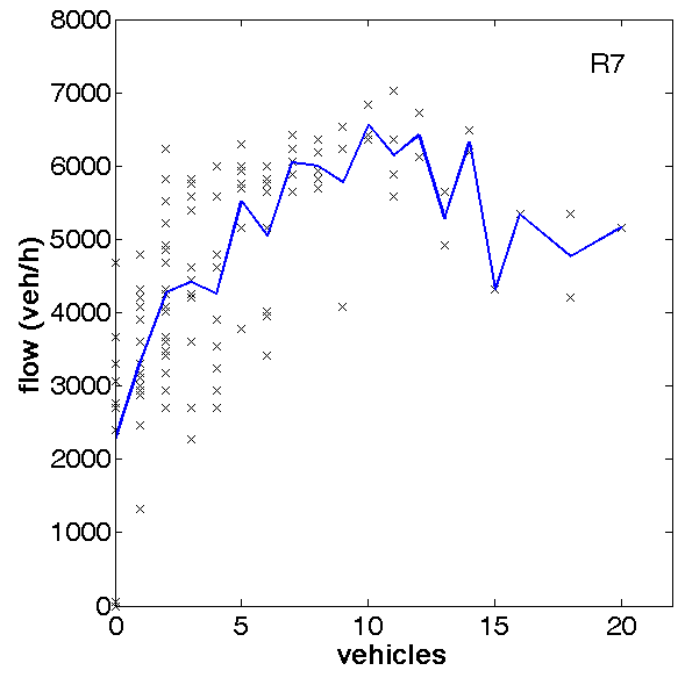


(b)

Figure 7-11: Merge area outflow (a) before the use of AFT and (b) after the use of AFT.

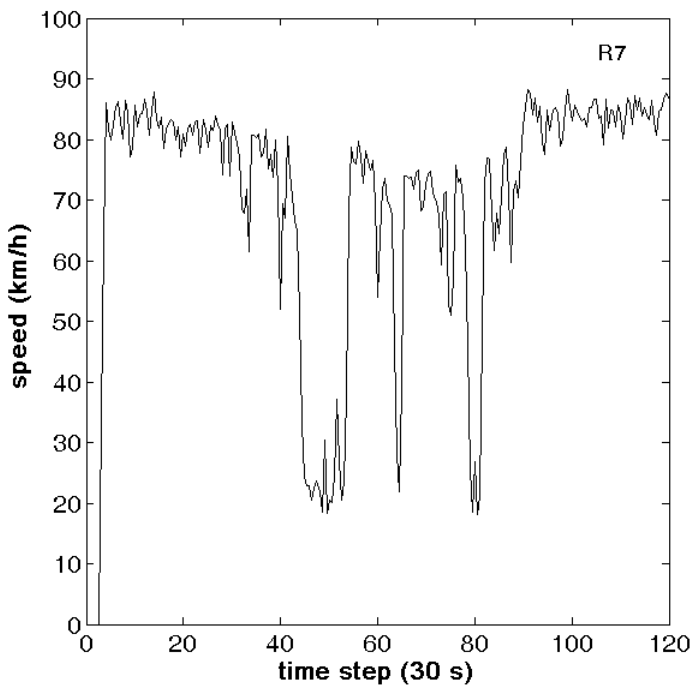


(a)

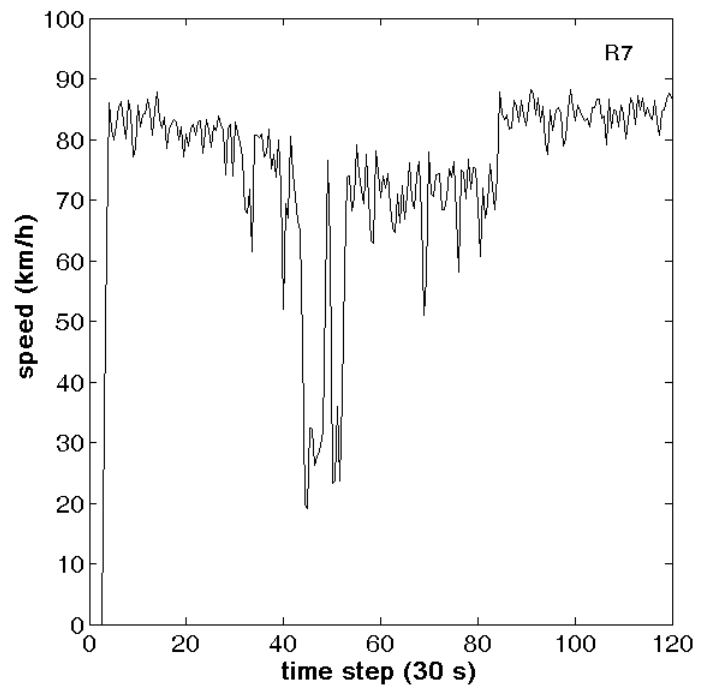


(b)

Figure 7-12: Outflow versus number of vehicles N (a) before the use of AFT and (b) after the use of AFT.



(a)



(b)

Figure 7-13: Speed upstream of the merge area (a) before the use of AFT and (b) after the use of AFT.

7.2.3 Control scenario 3

In the third control scenario the initial values for the tunable parameters are $K_P = 200 \text{ h}^{-1}$, $K_I = 50 \text{ h}^{-1}$ and $\hat{N} = 50 \text{ veh}$. These values correspond to a very “bad” set of regulator parameters and they are selected in order to investigate the reaction of the AFT algorithm and the values that it is going to converge to. Figures 7-14—7-17 display the resulting AVD values and the trajectories of the tunable parameters for two different AFT runs. As it can be seen in Figure 7-14, during the first iterations the AVD values are very high for both runs, however after the 20th iteration the AFT algorithm manages to keep the AVD at lower values. According to Figures 7-15—7-17 AFT algorithm converges in the first run to $K_P = 204.18 \text{ h}^{-1}$, $K_I = 31.32 \text{ h}^{-1}$ and $\hat{N} = 12.13 \text{ veh}$, while in the second run converges to $K_P = 289.9 \text{ h}^{-1}$, $K_I = 70.64 \text{ h}^{-1}$ and $\hat{N} = 11.76 \text{ veh}$. The values of K_P and K_I , for the first AFT run, are close to the initial ones (before the use of AFT), whereas the corresponding K_P and K_I values for the second AFT run are increased. It is noteworthy that the value \hat{N} is reduced a lot for both AFT runs and stabilizes at values very close to the best value derived from the manual fine-tuning ($\hat{N} = 11$).

Table 7-3 presents the AVD values for 10 replications for the initial control scenario (before the use of AFT algorithm) as well as the corresponding results for the the new control scenario derived from the first AFT run. As observed in the table, for the initial control scenario the AVD values for the 10 replications are very high with a mean AVD value equal to 35.66 s/veh/km. After the use of AFT the mean AVD value for the new control scenario is reduced about 57 %, which is a significant improvement of the system’s performance. For the second AFT run the resulting mean AVD value is reduced to 17.92 s/veh/km. However, this improvement is not sufficient as the fine-tuning of the control scenarios examined in the previous sections provide better improvement according to the mean AVD values (see Table 7-1 and Table 7-2).

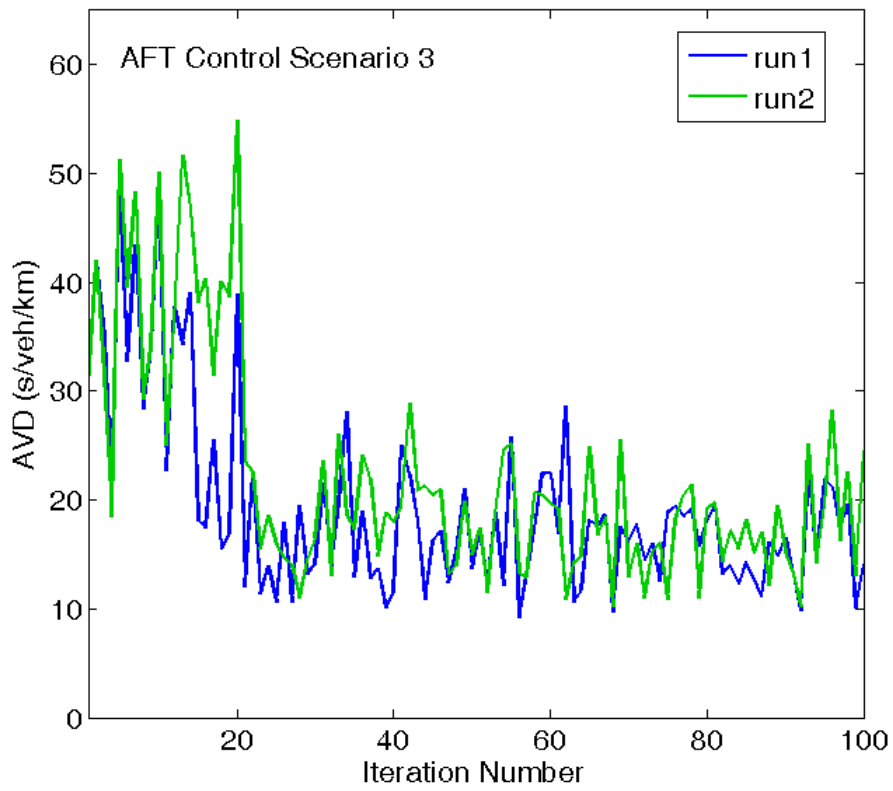


Figure 7-14: Average vehicle delay for control scenario 3.

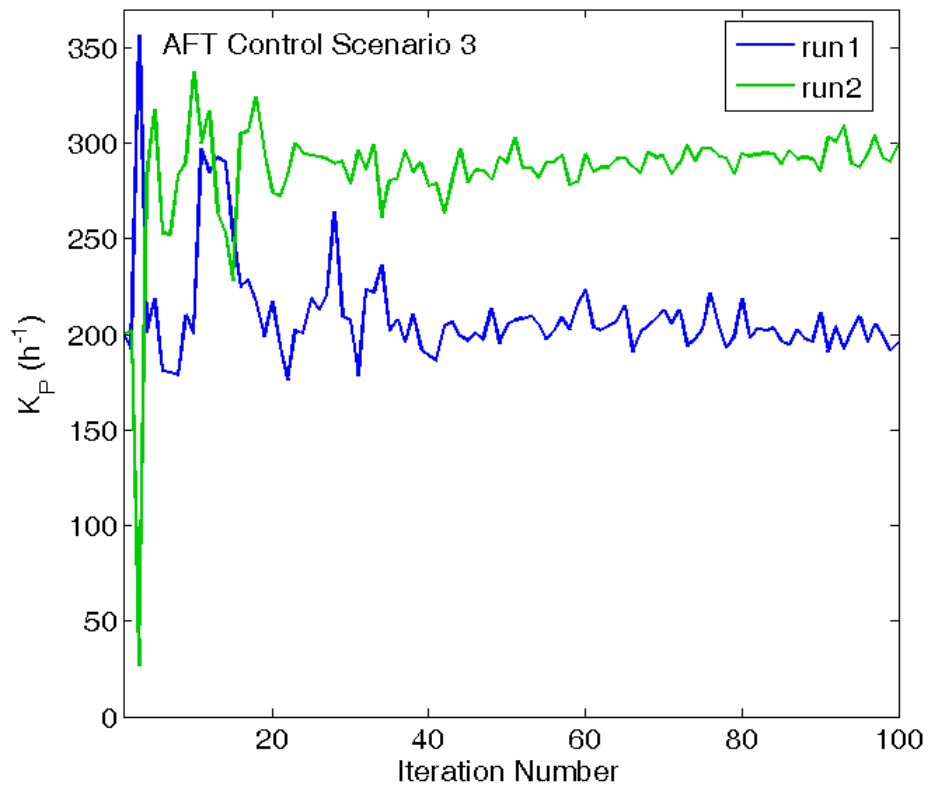


Figure 7-15: K_P parameter for control scenario 3.

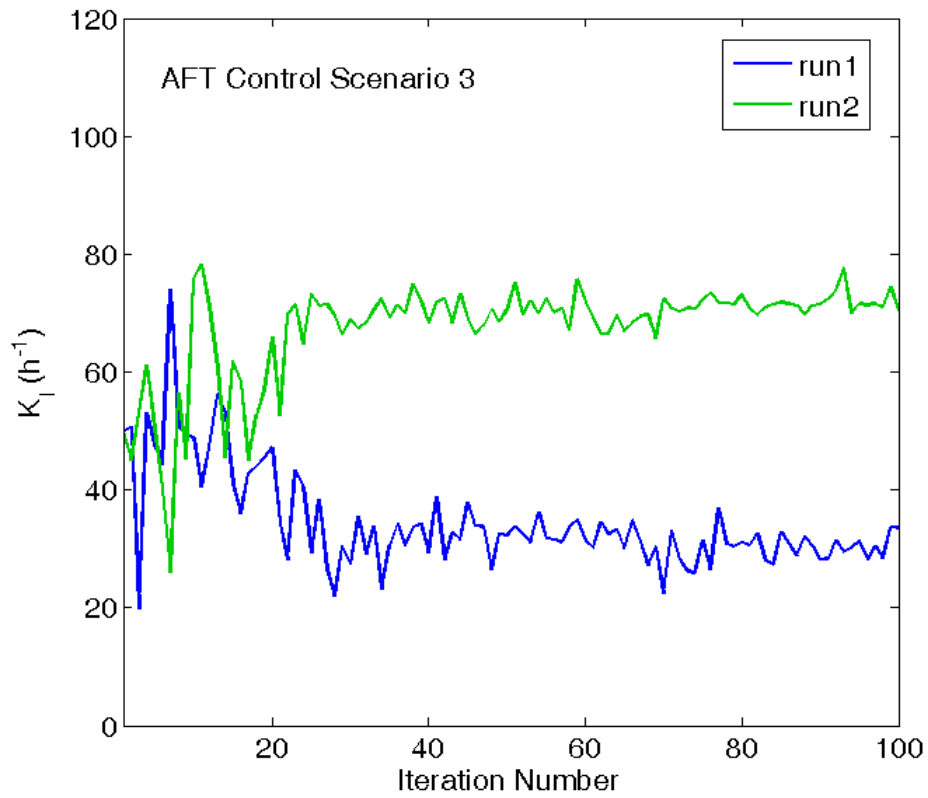


Figure 7-16: K_I parameter for control scenario 3.

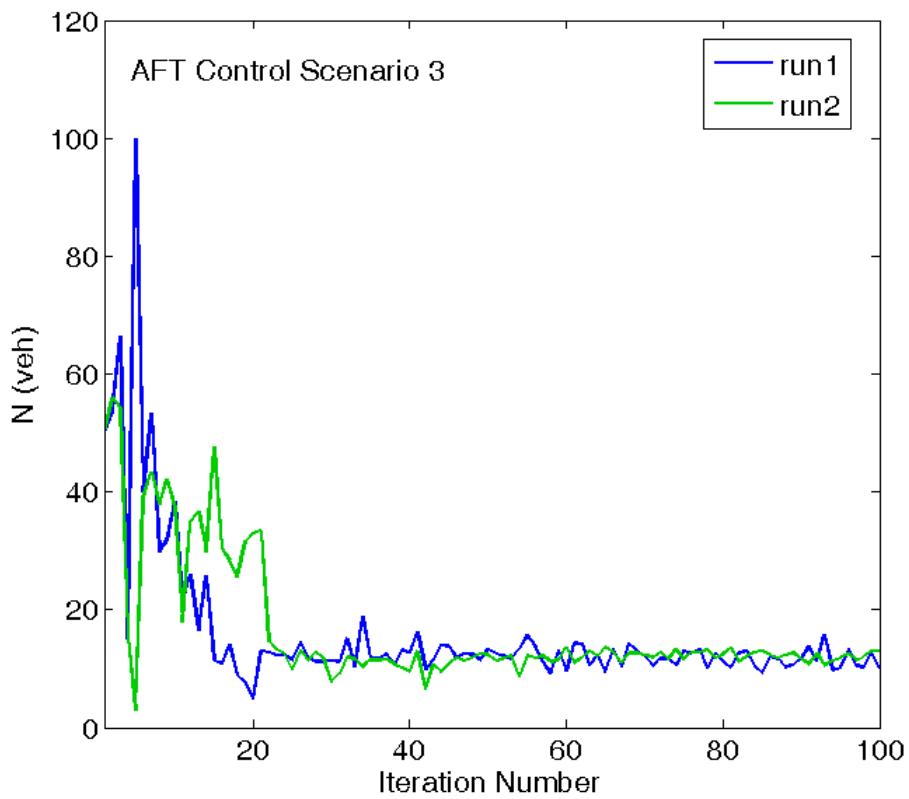


Figure 7-17: \hat{N} parameter for control scenario 3.

Table 7-3: Comparison of the average vehicle delay (AVD) with and without the application of AFT.

Replications	Before AFT	After AFT
	$K_p = 200, K_I = 50, \hat{N} = 50$ AVD (s/veh/km)	$K_p = 204.18, K_I = 31.32, \hat{N} = 12.13$ AVD (s/veh/km)
R1	38.12	12.01
R2	38.15	23.17
R3	48.37	17.67
R4	43.39	10.51
R5	30.48	11.99
R6	38.14	21.73
R7	23.53	12.40
R8	24.74	12.41
R9	42.11	18.80
R10	29.60	12.63
Average Value	35.66	15.33
Minimum Value	23.53	10.51
Maximum Value	48.37	23.17

It should be noted that in this case AFT algorithm provided sufficient improvement to the system's performance, although, it couldn't reach the AVD value of the previous experiments ($\cong 14$ s/veh/km). This is, due to the initial set values of the control scenario, which are considered as "bad" values. AFT converges to a closer local minimum value and stays there, and as a result the quality of the previous experiments cannot be achieved.

7.2.4 Control scenario 4 with fixed set point

In this experiment only two of the tunable parameters are selected to be fine-tuned by the AFT algorithm. The set point \hat{N} is considered constant and equal to 11veh, which is the selected value for \hat{N} derived by the manual fine-tuning procedure. The initial values for the tunable parameters K_p, K_I are selected equal to 150 h^{-1} and 6 h^{-1} , respectively, and are the optimized values delivered from the manual fine-tuning as well. Figures 7-18—7-20 display the resulting AVD values for two AFT runs and the trajectories of the tunable parameters. As observed in Figure 7-18, there is no actual reduction in average of the AVD values. In Figure 7-19 and Figure 7-20, the convergence of the AFT algorithm can be observed after the fine-tuning procedure of the regulator parameters K_p and K_I , respectively. The resulting values of the parameters provided by the AFT algorithm are $K_p = 123.52 \text{ h}^{-1}$ and $K_I = 4.23 \text{ h}^{-1}$ for the first run. In the second run the searching activity of AFT was limited in the same region and finally converged to values very close to the aforementioned ($K_p = 138.34 \text{ h}^{-1}$ and $K_I = 4.71 \text{ h}^{-1}$).

Table 7-4 displays the resulting AVD values for 10 replications after applying the initial control scenario (before the use of the AFT algorithm) and the corresponding AVD values for one of the new control scenarios after the system fine-tuning by AFT.

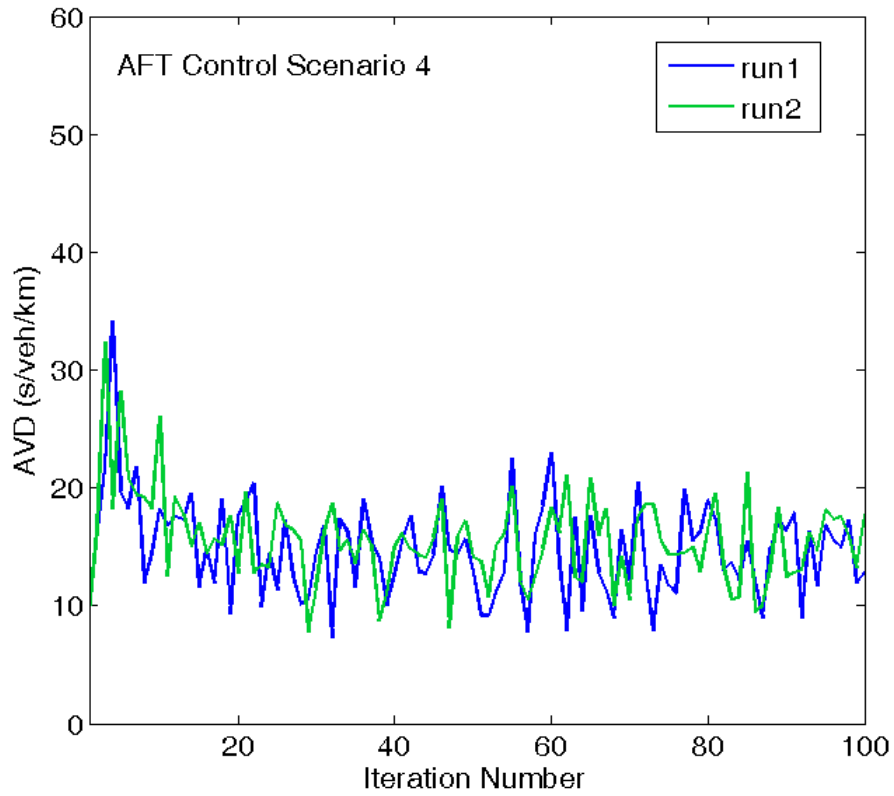


Figure 7-18: Average vehicle delay for control scenario 5.

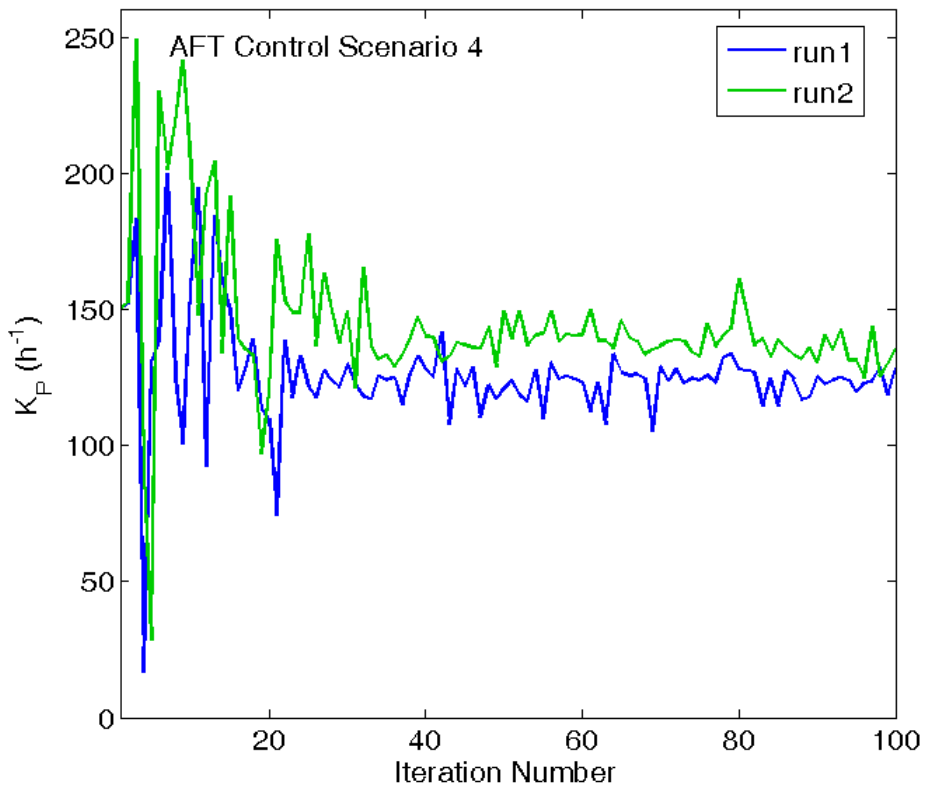


Figure 7-19: K_P parameter for control scenario 5.

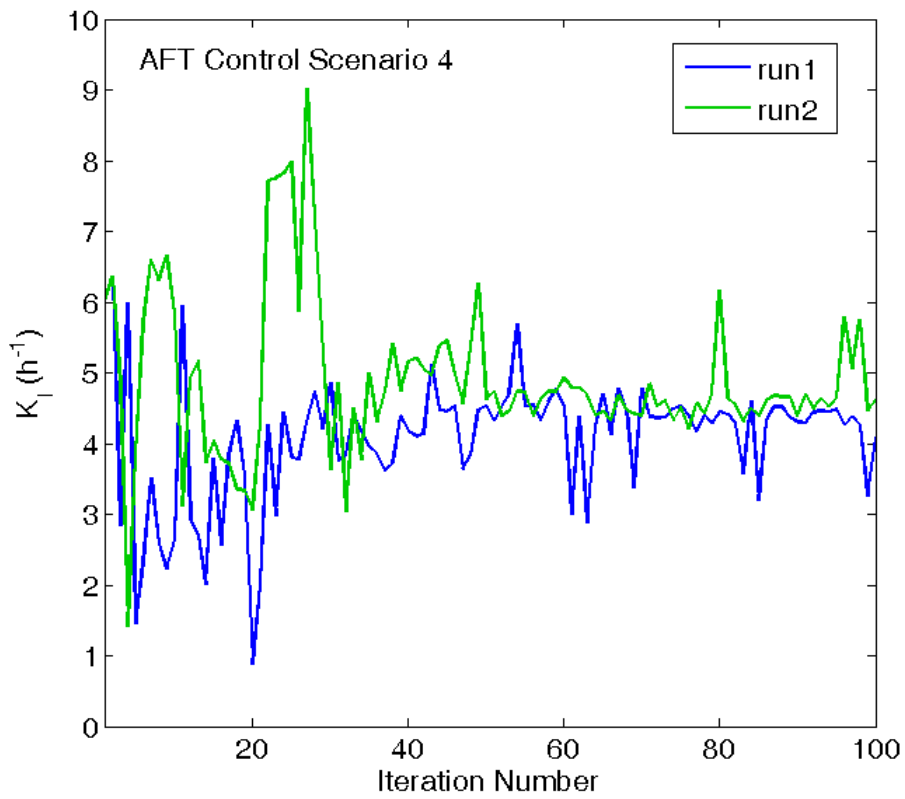


Figure 7-20: K_I parameter for control scenario 5.

Table 7-4: Comparison of the average vehicle delay (AVD) with and without the application of AFT.

Replications	Before AFT	After AFT (run 2)
	$K_p = 150, K_I = 6, \hat{N} = 11$ AVD (s/veh/km)	$K_p = 138.34, K_I = 4.71, \hat{N} = 11$ AVD (s/veh/km)
R1	12.43	12.40
R2	19.11	20.33
R3	15.70	13.80
R4	16.51	15.78
R5	9.44	11.41
R6	13.83	19.24
R7	11.58	10.52
R8	15.01	13.13
R9	18.45	17.52
R10	10.41	10.91
Average Value	14.25	14.50
Minimum Value	9.44	10.52
Maximum Value	19.11	20.33

As observed in Table 7-4 the resulting AVD values after the use of AFT are in average higher than the no AFT case. Furthermore, the AFT algorithm converges to a set of parameters very close to the manually optimized values; however, this does not enable the algorithm to efficiently fine-tune the regulator parameters. Probably, because of the fixed set point the feasible region in which the AFT algorithm is searching for a local minimum is limited and therefore it cannot achieve to optimize the overall system performance.

7.2.5 Application of AFT with Deviation Error of the regulator as the objective criterion

In this fine-tuning experiment the standard deviation of the regulation error $\sum(N - \hat{N})^2$ is used as the objective criterion to be optimized by the AFT algorithm. In this case, the parameters to be fine-tuned are only two, the K_p , K_I , whereas the set point (number of vehicles) is considered as a constant value. It is worth noting that the standard deviation error is calculated only for the “peak hours period” of the demand scenario with a duration of about 40 minutes.

For the calculation of the performance criteria (standard deviation of the regulation error and average vehicle delay), measurements are taken from detectors placed among the network (see Figure 5-2).

The selected initial values of the tunable parameters for this experiment are the ones that were derived via the manual fine-tuning procedure and are the

following: $K_P = 150 \text{ h}^{-1}$, $K_I = 6 \text{ h}^{-1}$ and the set point is set equal to $\hat{N} = 11 \text{ veh}$. Figure 7-29 displays the standard deviation error trajectory of the values delivered for one run of the AFT algorithm. Figures 7-26—7-27 display the trajectories of the same run for each tunable parameter of the system.

Although, as observed in Figure 7-21 the trajectory of the performance criterion fluctuates during the whole fine-tuning period, the AFT algorithm manages to reduce the standard deviation error. In Figures 7-22 and 7-23, it can be seen that the AFT algorithm converges to a set of parameters very close to the initial set values. Thus, no or slight additional improvement of the systems performance is expected. In order to assess the performance of the system, 10 simulation runs are carried out for the initial set values (before the use of the AFT algorithm), as well as for the set values at which the AFT algorithm converged. For the comparison of the two control scenarios, the AVD values are obtained and the simulation results are displayed in Table 7-5.

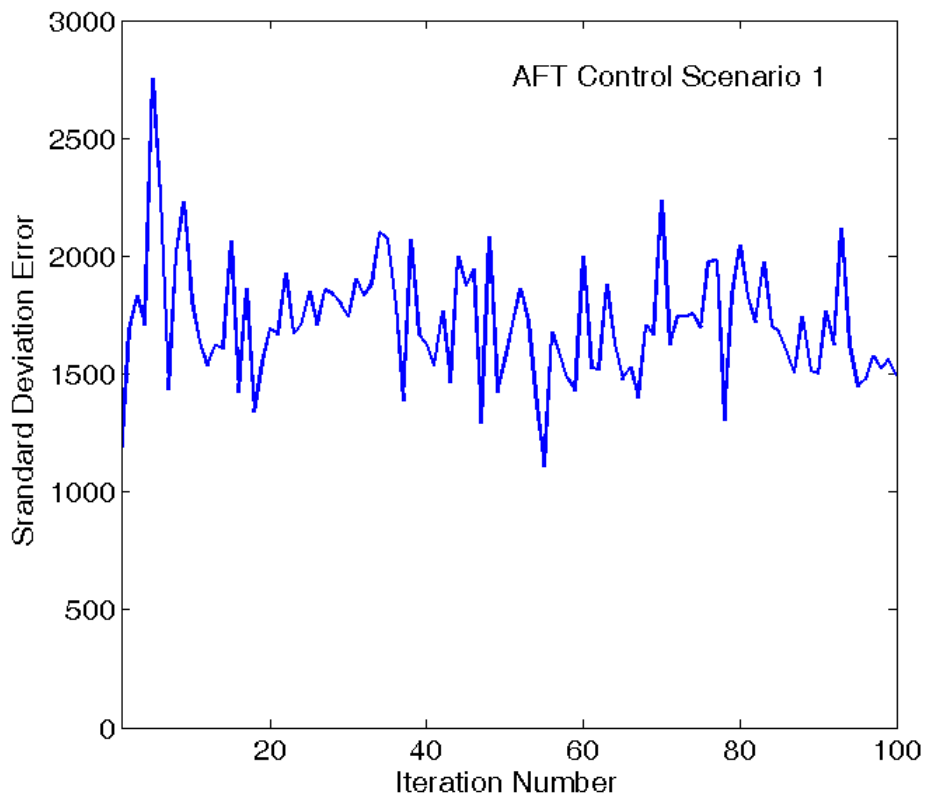


Figure 7-21: Standard deviation error for control scenario 1.

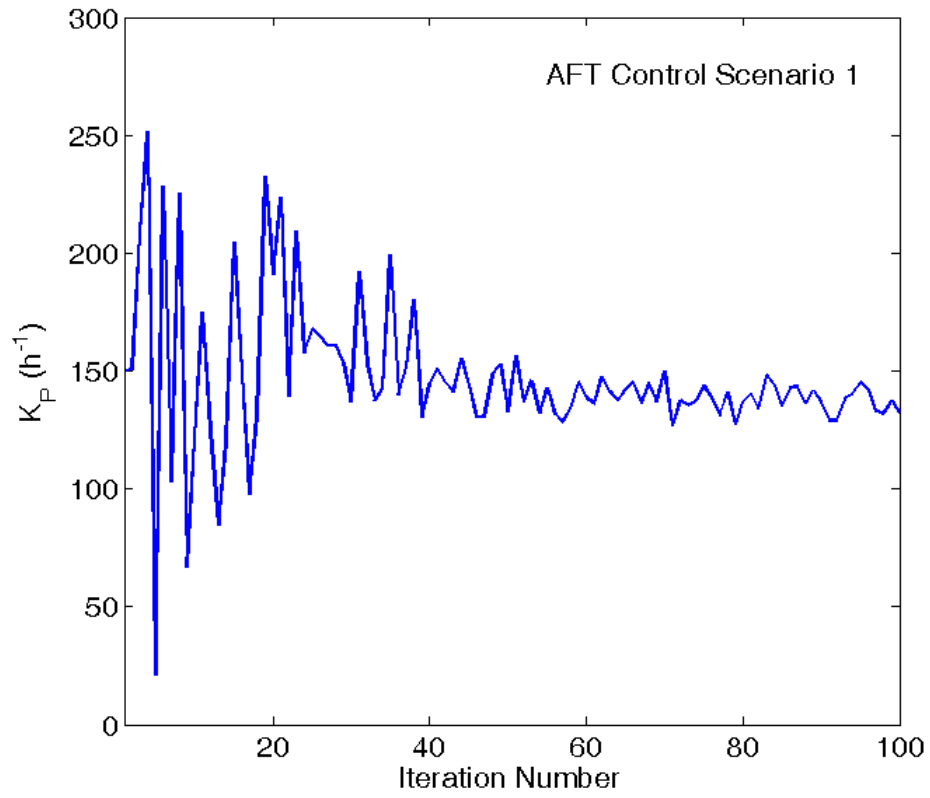


Figure 7-22: K_P parameter for control scenario 1.

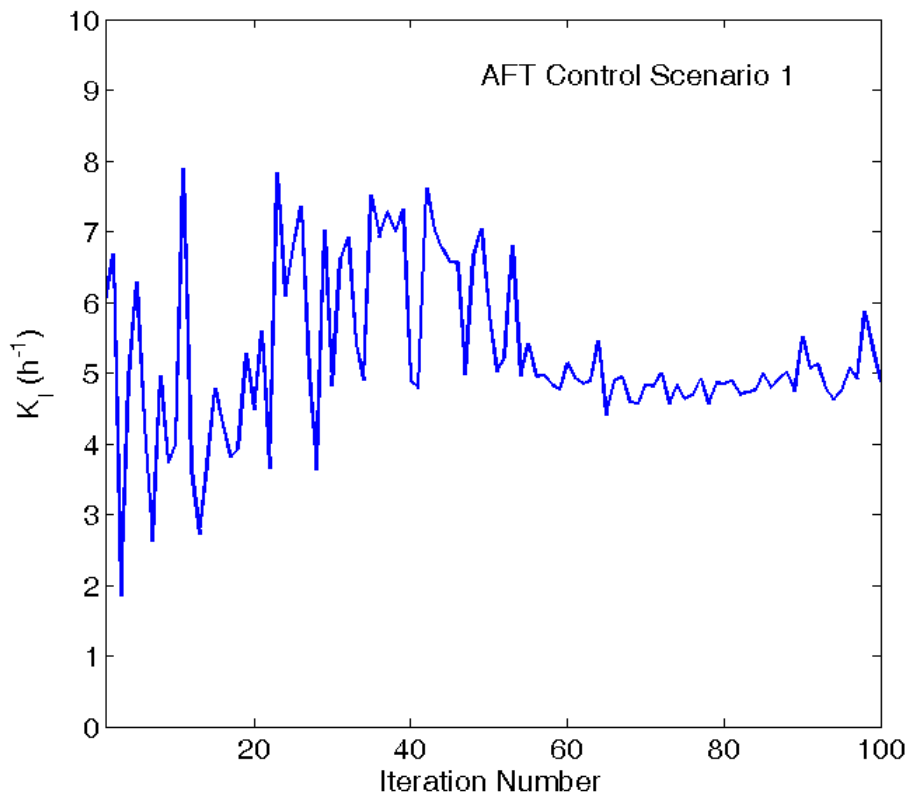


Figure 7-23: K_I parameter for control scenario 1.

Table 7-5: Comparison of the average vehicle delay (AVD) with and without the application of AFT.

Replications	Before AFT	After AFT
	$K_p = 150, K_I = 6, \hat{N} = 11$ AVD (s/veh/km)	$K_p = 138.03, K_I = 4.91, \hat{N} = 11$ AVD (s/veh/km)
R1	12.43	15.16
R2	19.11	17.50
R3	15.70	13.80
R4	16.51	14.92
R5	9.44	11.04
R6	13.83	19.24
R7	11.58	10.39
R8	15.01	12.10
R9	18.45	19.82
R10	10.41	8.77
Average Value	14.25	14.27
Minimum Value	9.44	8.77
Maximum Value	19.11	19.82

As observed in Table 7-5, there is no improvement in the system performance according to the mean AVD value for the implemented control scenario after the use of the AFT algorithm. Apparently, the selected objective criterion for this specific optimization problem may not be an appropriate criterion for an efficient fine-tuning by the AFT algorithm. Several other traffic related criteria should be taken into account in order to form an appropriate objective function. The minimization criterion used within the AFT algorithm should be always carefully chosen in order to include accurate knowledge of the traffic characteristics (i.e., vehicle speed, demand, delay etc.), otherwise the algorithm could lead to unacceptable results.

Finally, Tables 7-6 and 7-7 display the resulting AVD values of two more AFT experiments: (a) for a set of parameters with fixed set-point and (b) for a “bad” initial set of regulator parameters.

Table 7-6: Comparison of the average vehicle delay (AVD) with and without the application of AFT for a set of regulator parameters with fixed set-point.

Replications	Before AFT	After AFT
	$K_p = 200, K_I = 50, \hat{N} = 11$ AVD (s/veh/km)	$K_p = 194.42, K_I = 38.81, \hat{N} = 11$ AVD (s/veh/km)
R1	21.57	16.90
R2	19.97	16.28
R3	21.50	20.93
R4	16.07	12.25
R5	12.00	20.36
R6	17.28	16.06
R7	12.87	11.12
R8	13.42	16.30
R9	16.56	19.14
R10	10.78	9.30
Average Value	16.20	15.87
Min Value	10.78	9.30
Max Value	21.57	20.93

Table 7-7: Comparison of the average vehicle delay (AVD) with and without the application of AFT for a “bad” set of regulator parameters.

Repl.	Before AFT	After AFT (run 1)	After AFT (run 2)
	$K_p = 100, K_I = 60, \hat{N} = 30$ AVD (s/veh/km)	$K_p = 118.29, K_I = 99.58, \hat{N} = 10.06$ AVD (s/veh/km)	$K_p = 152.38, K_I = 15.67, \hat{N} = 10.63$ AVD (s/veh/km)
R1	38.12	14.90	12.70
R2	31.45	18.42	14.63
R3	48.37	18.95	14.65
R4	43.39	18.52	12.50
R5	30.48	12.00	15.89
R6	35.09	19.32	18.16
R7	23.53	15.08	12.24
R8	24.74	11.82	9.17
R9	42.03	24.51	20.25
R10	29.60	18.43	10.15
Avg.	34.68	17.19	14.03
Min.	23.53	11.82	9.17
Max.	48.37	24.51	20.25

8 Conclusions and future work

8.1 Thesis summary

In this research a control scheme was developed for real-time merging traffic control at work zones with lane drop, and was applied to a hypothetical work zone motorway infrastructure within a microscopic simulation environment. The control algorithm used for the work zone management was an extension of the well-known local ramp metering strategy ALINEA, while the control devices to implement the control algorithm decisions are traffic lights located sufficiently upstream of the work zone area. The current study addressed the appropriate distance between the traffic lights and the merge area, and demonstrated its significance for throughput maximization (or equivalently delay minimization) via avoidance of the capacity drop. All the simulation experiments are conducted via the microscopic simulator of road networks AIMSUN. A further investigation in this research was related to the fine-tuning procedure needed for the calibration of the control algorithm parameters. In particular, after the manually conducted fine-tuning procedure, the recently proposed learning/adaptive algorithm AFT was applied in order to seek for better regulator parameter values which lead to improved performance of the utilized control strategy.

8.2 Concluding remarks

The simulation results of the current investigation showed that the implementation of the PI-ALINEA control strategy in combination with the appropriate traffic lights position upstream of the merge area may improve the overall traffic conditions. In fact, it is shown that the average vehicles speed when reaching the merge area is significantly increased compared to the no-control case, while the average vehicle delay in the network is reduced and, equivalently, the exit flow from the merge area is increased. The investigation of the traffic lights location demonstrated that the distance between the traffic lights and the merge area affects the vehicles behavior and ability for proper acceleration so as to pass through the work zone efficiently.

Moreover, the described experiments for the application of the AFT algorithm show that the AFT algorithm can improve the system performance independently of the starting points. Nevertheless, the selection of, at least roughly, appropriate starting values for the regulator parameters (e.g. derived from manual fine-tuning) may be necessary in order to achieve best performance of the utilized control strategy. Moreover, as AFT does a “blind” optimization of the selected objective function, this function should be defined in a correct way, using all the necessary data. A bad

selection of the objective criterion could lead to results that do not correspond to the initial user objectives.

8.3 Future approaches

The results of this research are very promising and a potential field application of the presented control concept is expected to be successful. Moreover, the proposed control scheme could be suitable for other infrastructure layouts that may even not include a lane drop, such as tunnels and bridges where the motorway capacity may be reduced.

The AFT algorithm was efficiently applied and the produced simulation results may constitute real control schemes for future implementation at a work zone infrastructure. The significance of this investigation is that the AFT algorithm can be applied similarly in the field, based on real measurements, to optimize the control system performance.

Bibliography

- Burges, C. J. C., (1998). A Tutorial on support vector machines for pattern recognition. *Data Mining and Knowledge Discovery* 2, pp. 121-167.
- Carlson, R. C., Papamichail, I., Papageorgiou, M., and Messmer, A., (2010). Optimal mainstream traffic flow control involving variable speed limits and ramp metering. *Transportation Science*, 18, pp.193-210.
- FHWA, (2005). *Developing and Implementing Transportation Management Plans for Work Zones*. Report of the Federal Highway Administration, U.S.. Department of Transportation.
- Giannakis, G. I., Kontes, G. D., Kosmatopoulos, E. B., Rovas, D. V., (2011). A model-assisted adaptive controller fine-tuning methodology for efficient energy use in buildings. *19th IEEE Mediterranean Conference on Control and Automation*, Corfu, Greece, June, pp. 49-54.
- Kouvelas, A., (2011). *Adaptive Fine-Tuning for Large-Scale Nonlinear Traffic Control Systems* (PhD thesis). Technical University of Crete, Chania, Greece.
- Kouvelas, A., Aboudolas, K., Kosmatopoulos, E. B., and Papagorgiou, M., (2011). Adaptive performance optimization for large-scale traffic control systems. *IEEE Trans. on Intelligent Transportation Systems*, to appear (DOI:10.1109/TITS.2011.2159002).
- Lentzakis, A. F., Spiliopoulou, A. D., Papamichail, I., and Papageorgiou, M., (2008). Real-time work zone management for throughput maximization. *87th Transportation Research Board Annual Meeting*, Washington, DC, January 13-17, paper 08-0772.
- Lin, P. W., Kang, K. P., and Chang, G. L., (2004). Exploring the effectiveness of variable speed limit controls on highway work-zone operations. *Journal of Intelligent Transportation Systems*, 8, pp. 155-168.
- Papageorgiou, M., Haj-Salem, H., and Blosseville, J-M.,(1991). ALINEA: A local feedback control law for on-ramp metering. *Transportation Research Record* 1320, pp. 58-64.
- Papageorgiou, M., Haj-Salem, H., and Middelham, F., (1997). ALINEA local ramp metering: summary of field results. *Transportation Research Record* 1603, pp. 90-98.
- Papageorgiou, M., and Papamichail, I.,(2008). Overview of traffic signal operation policies for ramp metering. *Transportation Research Record* 2047, pp. 28-36.
- Papageorgiou, M., Papamichail, I., Spiliopoulou, A. D., and Lentzakis, A. F., (2008). Real-time merging traffic control with applications to toll plaza and work zone management. *Transportation Research Part C*, 16, pp. 535-553.
- Papageorgiou, M., and Kotsialos, A., (2002). Freeway ramp metering: an overview. *IEEE Trans. on Intelligent Transportation Systems* 3, pp. 271-281.
- TSS-transport simulation systems, (2009). *Aimsun Users Manual Version 6*.
- Vigos, G., Papageorgiou, M., and Wang, Y., (2008). Real-time estimation of vehicle-count within signalized links. *Transportation Research Part C*, 16, pp. 18-35.
- Wang, Y. , and Papageorgiou, M., (2006). Local ramp metering in the case of distant downstream bottlenecks. *IEEE Intelligent Transportation Systems Conference*, Toronto, Canada, September 17-20.
- Wei, H., and Pavithran, M., (2006). Concept of dynamic merge metering approach for work zone traffic control. *11th IFAC Symposium on Control in Transportation Systems*. Delft, The Netherlands, August 29-31, pp. 374-379.